INVESTIGATIONS OF THE CHEMICAL COMPATIBILITY OF RHENIUM WITH URANIUM DIOXIDE AT ELEVATED TEMPERATURES

By

DJAMEL KAOUMI

A THESIS PRESENTED TO THE GRADUATE SCHOOL
OF THE UNIVERSITY OF FLORIDA IN PARTIAL FULFILLMENT
OF THE REQUIREMENTS FOR THE DEGREE OF
MASTER OF SCIENCE

UNIVERSITY OF FLORIDA

2001

To Ourdia Alouache

ACKNOWLEDGMENTS

I would like to thank Dr. Samim Anghaie for supporting me during these two years at INSPI. His trust and encouragement were very much appreciated. I would like also to thank Dr. Edward T. Dugan for his support and for being so available as a teacher throughout my graduate work at the University of Florida. I am grateful to Dr. Rajiv K. Singh from the Materials Sciences and Engineering department for his support as a teacher and for taking time to be part of my committee. I would also like to thank everyone at INSPI (Lynne, Travis, Blair, Gary, Vadi) for their valuable help and kindness and for the agreeable ambiance. I would also like to thank my mother and family for their continuous support, and my friends whose support was very encouraging.

TABLE OF CONTENTS

page

APPENDICES

LIST OF TABLES

Table page

LIST OF FIGURES

Abstract of Thesis Presented to the Graduate School
of the University of Florida in Partial Fulfillment of the
Requirements for the Master of Science

INVESTIGATION OF THE CHEMICAL COMPATIBILITY OF RHENIUM WITH URANIUM DIOXIDE AT VERY HIGH TEMPERATURES

By

Djamel Kaoumi

August 2001

Chairman: Samim Anghaie
Major Department: Nuclear and Radiological Engineering Department

Because of its high melting point, outstanding ductility, good strength and creep behavior, rhenium has been a very good candidate for high-temperature applications in the field of aerospace. It is particularly suitable for application as structural material in space nuclear reactor cores. Rhenium is also proposed as fuel cladding material for high temperature space reactors. It has also been proposed as a liner for the fuel pin in a space power reactor design (SP-100 program) because of its high neutron absorption cross section that could make the reactor subcritical under a hypothetical water submersion accident. Despite all positive high temperature properties, Rhenium lacks corrosion resistance in the oxidation environment. As a cladding material for uranium dioxide fuel pellets, no chemical interaction between the two materials is acceptable. The purpose of

this study is to investigate chemical compatibility between urania and rhenium at elevated temperatures.

The “F*A*C*T” code was used to determine from a thermodynamic point of view the chemical equilibrium composition of a UO_2/Re system in the range of temperatures [2000 K – 3000 K]. The code results, which were based on calculations of Gibbs free energies, have shown no chemical interaction between the two species in the temperature range of interest. This is evident because uranium dioxide is much more stable than any of the possible chemical products involving rhenium.

An induction-heating furnace was used to sinter mixtures of uranium dioxide and rhenium powders for 10 hours, at temperatures as high as 2500 K. This temperature is much higher than the intended design temperature for which rhenium is a candidate. The x-ray powder analysis technique was used to analyze the samples prior to and after the sintering process. Back-scattered scanning electron imaging was used to complement the x-ray analysis when relevant. The results led to the conclusion that rhenium and uranium dioxide do not chemically interact at temperatures as high as 2500 K.

CHAPTER 1
INTRODUCTION AND BACKGROUND

Rhenium (Re) was discovered in June 1925 by Walter and Ida Noddack (husband and wife). Since then, the interest in this metal has never slowed down. However, its scarcity and high cost prevented it from being used extensively in large structural components (especially in its pure form). The rapid development of this recently discovered element is actually due to its very unique combination of physical and mechanical properties. However, rhenium has been used as an alloying element for a long time now because of its positive effects on other refractory metals. Those refractory metal alloys have been used as heating elements, high-temperature thermocouples, anti-friction and low wear parts, compact electromagnet coils, and high-temperature elastic elements. Because of their unique properties, rhenium and its alloys have been considered for many applications in the field of aerospace.

The SP-100 Program is one of them [1]. This program was an aerospace project of high-temperature liquid-metal-cooled nuclear power plant; it was designed to provide tens to hundreds of kWe power for 7 years at full power and 10 years of overall operation. The clad provided structural strength for the fuel pin, which was the heart of the reactor design. The layer of rhenium was designed to prevent interaction with fuel. It also allowed thinner cladding, and would act as a thermal poison if the reactor was immersed in water because of its high neutron capture cross-section in certain conditions. As for the fuel pin cladding material, it was niobium alloy PWC-11. These structural materials were needed to meet important requirements involving their physical,

mechanical, thermal, and chemical properties. For the SP-100 program in particular, the structural elements had to show good resistance to corrosion by liquid alkali metal coolants and good compatibility with candidate fuel materials such as uranium dioxide (UO_2). To date, little work has been done in this area. The chemical compatibility of rhenium (Re) with UO_2 at very high temperatures has never really been studied for itself, and was the object of this investigation. However in the past, some experiments involved rhenium and UO_2 as part of their materials; they are briefly reported below.

The 710-Reactor Program

During the 710-space-nuclear-reactor program initiated in the 1960s, UO_2 was chosen as the most probable reactor fuel because it had the highest melting point of all potential fuel candidates at that time and because it had the lowest vapor pressure at high temperature. Moreover, the technology for processing UO_2 had benefited from years of experience in the nuclear industry, which made it readily available commercially. During further development of the fuel program, it was established that UO_2 could be combined with W to form a cermet (ceramic-metal) material: a W matrix encasing fuel particles. A UO_2-(40 vol %)W cermet system was achieved and showed high strength, adequate ductility, and thermal conductivity one order of magnitude higher than that of UO_2 alone. Later rhenium was added to the matrix to improve the ductility of the fuel. The final matrix needed to be contained in a cladding. And of course the choice of the cladding material was the first question to be solved.

The structural material supporting and containing the fuel matrix needed special properties such as a high melting point for structural integrity, low vapor pressure,

adequate ductility, a fabricability to close-to-dimensional tolerances, good strength, and of course compatibility with the nuclear fuel and the coolant. Based on these requirements, refractory metals appeared to be the most advantageous materials for structural applications because they combined the above properties and were most likely to be compatible with UO_2. Some of these refractory metals were also compatible with H_2 and liquid metals, which made them very good candidates for the 710-fuel program. Many possibilities were considered before actually choosing the final cladding materials that would be tested. Tungsten had the highest melting point (3410 °C) and the lowest vapor pressure of all the possible refractory structural materials but it had low ductility and poor grain boundary strength, thus enhancing grain boundary diffusion, which constituted a problem for high temperature and partial pressure UO_2 in a thin tungsten (W) structure.

A tungsten-based alloy such as W-Re was then considered to be the best cladding candidate from the very beginning but because it was not commercially available at that time (1961) in the required sizes and shapes, other materials were selected for the initial development work. Nevertheless, research work on W-Re alloy was initiated in parallel so that in 1964 it resulted in the production of two W-Re-Mo alloys. Further studies in the 710-reactor program on systems using those alloys as the cladding material were achieved. Tantalum was also considered for cladding purposes because it had the highest melting point of the refractory metals commercially available at that time (1961), and it could be fabricated in the wanted shapes and sizes, and it also had good high-temperature material properties. A Ta-(10 vol %)W alloy was also available commercially in fabricated shapes and dimensions required for the 710 program; it had mainly the same

properties as Ta with better stress-rupture properties. Molybdenum and Niobium were also available in the desired shapes but their relatively low melting point constituted a drawback.

Henceforward, early work on the 710-reactor program concentrated on Ta and Ta-10W cladding materials. Work was also conducted on two W-Mo-Re alloys: (W-30Re-30Mo, at%), and (W-25Re-30Mo, at%). In 1962, a better tantalum alloy called T-111 (Ta-8W-2.4Hf, wt%) became available commercially and was tested as well. Testing all these different materials actually allowed the scientists to compare them and see how all of them behave in contact with the W-UO_2 matrix. The results and conclusions of relevance to this thesis are presented below.

For the Ta-clad/W-UO_2 system with hyperstochiometric UO_2 fuel, post-test metallographic and microbeam analyses showed the formation of TaO_5 in the cladding.

As for the studies involving T-111 alloy, they showed that W-UO_2 cores with O/U ratios not less than 2.00 before cladding in the T-111 alloy had substochiometric O/U ratios after hot-gas pressure bonding for 3 hours at 3180 °F in a 10000-psig helium atmosphere. Further metallographic, microprobe, and chemical analyses of the cladding showed that this reduction in stochiometry was due to oxygen gettering by hafnium contained in the T-111 alloy since HfO_2 was detected in the grain boundaries and within grain bodies of the cladding.

The W-Re-Mo alloy was first used in a study on the dimensional stability of the fuel where W-Re-Mo capsules enclosing W-UO_2 with different initial O/U ratios were cycled from 500 °F to 3000 °F. Two of the supposedly initially hyperstochiometric capsules were submitted to metallographic and chemical analysis. The analysis showed

no presence of free uranium and a stochiometric O/U ratio. But microprobe analysis detected grain boundaries stringers of WO_2 in the W matrix. These WO_2 stringers seemed to alter the dimensional stability of the cermet by raising the ductile-to-brittle transition temperature of the W matrix by dissociation to gaseous WO_3 and by forming UO_2-U_xWO_3 eutectic phases. The discovery of WO_x phases within the cores clad in W-Re-Mo led to an actual study of the compatibility of W-Re-Mo cladding with UO_2 and UO_{2+x} at 3000 °F. Two capsules were prepared: one contained a core sintered in conditions leading to an O/U ratio of 2.003±0.004, the other was spiked with U_3O_8, which resulted in an O/U ratio of 2.026. Both capsules were electron-beam welded in vacuum and heated in argon at 3000 °F for 70 hours. In both cases, the clad disclosed oxide precipitates of various colors: gold, blue, violet, brown; however, the clad of the hyperstochiometric core showed much greater amounts of oxide deposits. Its X-ray diffraction examination indicated the presence of WO_2 and MoO_2, a perovskite-type bronze (possibly U_xWO_3), UO_2, and W metal. Electron probe analysis of metallographic sections detected mixed W-Mo oxides on the cladding of the stochiometric capsule, and a mixture of three oxide phases, which was a liquidus grain boundary phase containing W and U with lower mass density than UO_2. It was presumed to be W-U oxide. Analysis showed an increase of the level of oxygen in both claddings. Based on these results it could be concluded that reactivity can occur between W-Re-Mo clad and $UO_{2.026}$ and that some interaction is even possible between the W-Re-Mo cladding and $UO_{2.003}$.

These tests actually showed that all of the refractory metals of interest (W, Ta, Hf) chemically interacted with UO_2 (even though the temperatures were not ultra-high), except Re. It is important to note that absolutely no interaction between Re and UO_2 was

mentioned in the reports. However it is also important to note that in all the experiments, Re was always present in minor quantities, as an alloying element in materials involving other refractory metals, never as a pure cladding element [2].

Latta's Study on Solidus Liquidus Temperatures of $UO_{2\pm x}$

In 1969, R. E. Latta and R. E. Fryxell worked on the "determination of solidus-liquidus temperatures in the UO_{2+x} system ($-0.50<x<0.20$)" using sealed tungsten capsules to contain the urania [3]. But they also used rhenium capsules since this metal was known to be quite inert to uranium and had a very low oxygen permeation rate. They mentioned that Re dissolved in stochiometric UO_2 and that for oxygen-excess compositions, i.e. hyperstochiometric urania, the interaction was much more extensive. It is important to note that Weidenbaum and Haussner had previously raised the problem of tungsten dissolving in stochiometric urania; they had reported that tungsten dissolved in melt up of urania to a few tenths of a weight percentage and equilibrated within a few minutes. They observed that the hyperstochiometric urania which melted in tungsten presented rather large amounts of metallic tungsten and a violet or blue precipitate which was identified as a ternary oxide with perovskite structure U_xWO_3 (x having a value near 0.10). This was of course accompanied with a change in the urania composition, which finally got stochiometric. As for the rhenium capsules, they showed that molten hyperstochiometric urania dissolved rhenium which precipitates during cooling as pure metal in which no uranium was detected, leaving the urania with its initial O/U ratio. It goes without saying that the dissolution of the structural elements is to be avoided, as is the melting of the fuel that this implies [3].

Based on these studies, it could be stated that problems of chemical compatibility with uranium dioxide do occur for all other refractory metals (hafnium, molybdenum, and the widely utilized tungsten) except for rhenium: no chemical interaction was noted between rhenium and uranium dioxide. However, it must be noted that none of the studies quoted above were focused on the particular issue of the chemical compatibility of rhenium with urania. It was not the purpose of the study done by Latta, and even during the 710-reactor program when studies on the chemical compatibility between the cladding material and the UO_2 fuel were done; rhenium was only used in minor quantities, as an alloying element in the cladding material, never in its pure form. Hence, investigations needed to be done on this issue; especially since pure rhenium is seriously considered as necessary for lining the fuel pin in space power reactor programs. Therefore the purpose of this work was to investigate the compatibility of pure rhenium with urania at very high temperatures. The next chapter of this thesis addresses the physical, material, and chemical properties of rhenium, and describes its special features for high-temperature applications, such as in space power; it shows what makes rhenium such a unique material. The following chapter presents the theoretical and experimental work achieved, as well as the results, conclusions, and discussions.

CHAPTER 2
RHENIUM

Rhenium is a unique metal. Rhenium was discovered in 1925 in Germany but its production began only in 1948 in the former Soviet Union, and in East Germany and USA during the 1950s. Research in the area of treatment, properties, phase diagrams, and the design of rhenium alloys was initiated in the 1960s in the USA, Soviet Union, United Kingdom, Germany, France, and Poland. Rhenium belongs to the family of the refractory metals. This term refers to metals with a very high melting point, but it is somewhat used arbitrarily in the metals industry. For instance, the Refractory Metals Committee, organized under the Metallurgical Society of the American Institute of Mining, Metallurgical and Petroleum Engineers, uses the term refractory to cover only metals with a melting temperature above about 1900 °C. However, in the Metals Handbook published by the American Society for Metals, the refractory metals are those "metals having melting points above the range of iron, cobalt and nickel". The main refractory metals of interest for space nuclear power are those with the highest melting point: tungsten, rhenium, molybdenum, tantalum, niobium, hafnium, iridium…The particular combination of desirable properties of rhenium for high-temperature industrial applications makes it special. Because of its very high melting point, its high neutron capture cross section, and its numerous very good mechanical properties, rhenium was early considered as a very good structural material candidate in the aerospace industry for complex nuclear reactor core designs (SP-100 program, 710-high-temperature-gas-reactor program). However, because of its scarcity and its cost, pure rhenium had barely

been used in experimental work so far. Nowadays, tremendous advancements have been achieved due to the never-ending interest the scientific community has had in this material. This led to an increased commercial availability and a better knowledge of its unique combination of properties, which are described in this chapter [4, 5].

Rhenium's Physical Properties

Rhenium has an hexagonal close-packed lattice whose lattice parameters depend on the purity of the material: a = 0.2753-0.2765 nm, c = 0.4445-0.4480 nm, and c/a = 1.6147-1.6160. It retains its structure to its melting point (3180ºC), which is the second highest melting temperature of all refractory metals, after tungsten (3380ºC). This parameter decreases with addition of any impurity including tungsten.

Rhenium has a low thermal expansion coefficient ($6.7x10^{-6}$ K^{-1}), and a low vapor pressure at its melting point. As a dense metal (21.0 g/cm^3), it is only surpassed by osmium (22.6 g/cm^3), iridium (22.56 g/cm^3), and platinum (21.4g/cm^3). The boiling temperature of rhenium is 6173 K, which is equal to that of tungsten and exceeds those of other metals. The vaporization rate of rhenium is $8.41x10^{-6}$ g m^{-2} σ^{-1}. The maximum operating temperature at which the weight loss caused by vaporization does not exceed 1% after 10 h is 1910°C for molybdenum, 2380°C for rhenium, and 2560°C for tungsten. The thermal conductivity of 71.2 W/m K is approximately 2, 3, and 5.5 times smaller than that of Mo, W, and Cu, respectively. The linear thermal expansion coefficient (LTEC) of polycrystalline rhenium is $6.7x10^{-6}$ K^{-1}, which is somewhat low but still larger than that of Mo and W.

The high specific electrical resistance of rhenium (ρ) depends on the purity and on the degree of deformation of the material; ρ is 17.2 $\mu\Omega$ m for pure rhenium processed

by zone electron-beam melting and containing (in wt %) 0.0021 O_2, 0.0005 H_2, and 0.0006 N. For rhenium processed by vacuum arc melting and containing an increased amount of O_2 (0.0081-0.022 wt %), ρ is 18.75-22.85 μΩ m. For recrystallized rhenium processed by traditional methods of powder metallurgy, this parameter is 19.4 μΩ m. An addition of group-IV-VI transition metals into rhenium increases its specific electrical resistance.

With a value of ~10^{-16} - 10^{-11} at temperatures in the range of 1800 - 2400 °C, the self-diffusion coefficient of rhenium is close to that of W and Ta and is lower than that of other metals and alloys.

Ductility of Rhenium

Refractory metals are usually divided into two groups: the Group VA elements include Ta, Nb, and V, whereas the Group-VIA elements include Mo, W, and Cr. All elements of the Groups VA and VIA having a bcc lattice structure exhibit a ductile-to-brittle fracture transition behavior temperature. This temperature is higher for the Group VIA elements Cr, W, Mo than for the Group VA elements that exhibit a ductile-to-brittle transition temperature well below room temperature. Pure tantalum is ductile in tensile testing at 4.2 K. Figure 1 shows this ductile-to-brittle transition behavior for the refractory metals. Rhenium does not appear on the figure because it is the only refractory metal that is ductile in the entire range of temperatures, which makes it a very recommended material for cladding purposes. Research found that the addition of rhenium to the Group VIA elements lowers their ductile-to-brittle transition temperature to below room temperature, which is known as the “rhenium ductillizing effect”.

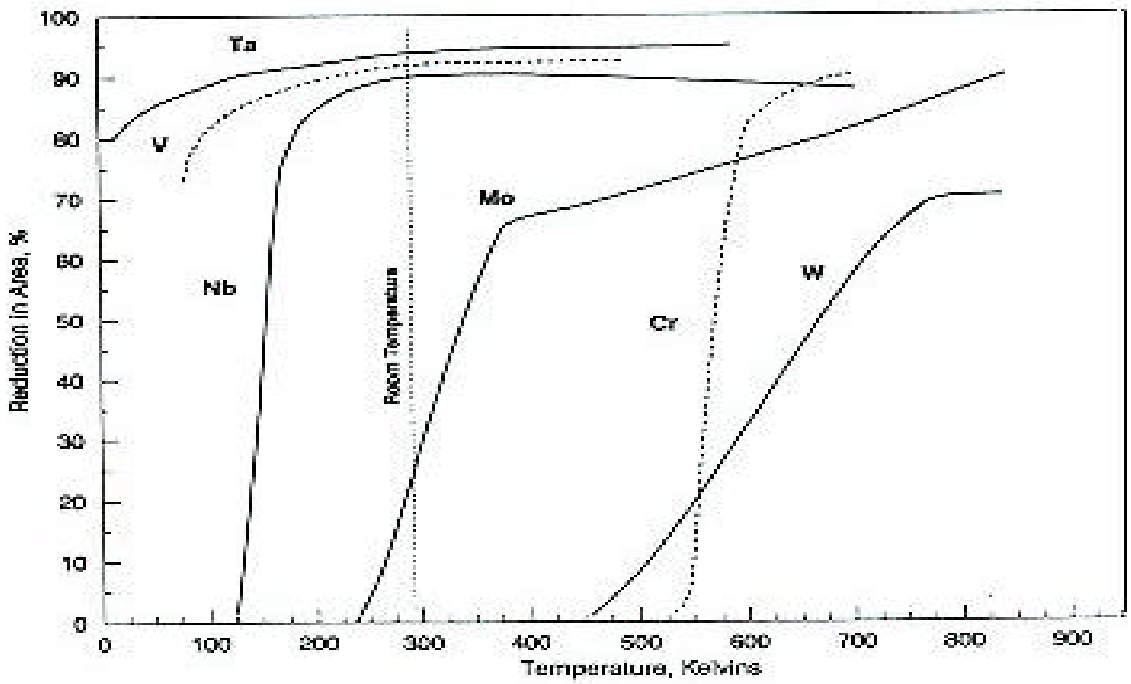

Figure 1: Ductile-to-brittle transition behavior of refractory metal versus temperature .

Workability of Rhenium

Rhenium can be cold worked or warm worked under vacuum. The deformation resistance of rhenium sharply increases after small deformation ($\varepsilon \sim 5\%$). The strain hardening rate estimated from the slopes of the "true stress – strain" curves of rhenium is 3.5 times higher than those of W and Mo. Rhenium has a strong strain hardening even when working at 1350°C. The observed hardening effect is caused by limited plastic deformation of the grain core associated with heavy twinning. Under industrial conditions, rhenium may be subjected to cold rolling and/or drawing to ε=10-15% between intermediate annealings without cracking.

Alloying with molybdenum and tungsten decreases the ability of rhenium to strain harden and actually improves its workability: rhenium containing 5-10 atomic percent of

Mo may be cold-worked without cracking to the degree of reduction of 30-40%. The workability of rhenium is unaffected by tantalum addition but deteriorates with the additions of zirconium and hafnium. An addition of ThO_2 to rhenium increases its strain-hardening rate [4].

Fabrication of Rhenium Parts

Since rhenium has great ductility, it is generally fabricated by cold-working and can be rolled into thin sheet, swaged and drawn into wire or tubing. The problem is that rhenium also has an important resistance to deformation and becomes very work-hardened even after cold-deformation of only a few percent. Its work hardening rate is higher than any other pure metal known. The tensile strength and ductility of processed rhenium parts vary as a function of the degree of cold-working applied to the parts; this phenomenon is more obvious than for any other pure metal. Cold-worked rhenium is also very tough and abrasion-resistant and can be used as a wear resistant material. In order to solve the problem of work-hardening, recrystallization or stress relief annealings are necessary at temperatures of 1500-1900 K in a vacuum or in an atmosphere of dry hydrogen or a hydrogen-nitrogen mixture follow each operation of cold-working. Besides eliminating the work-hardening, these operations also decrease the resistance to deformation. And unlike tungsten, for which recrystallisation results in extreme brittleness at room temperature, rhenium has a good ductility in both recrystallized and cast conditions [6].

Physicomechanical Properties of Rhenium

At room temperature, the elastic modulus of rhenium is as high as 460-510.3 GPa. This value is somewhat lower than those of osmium and iridium (570 and 538.3 GPa, respectively) but exceeds those of tungsten (420 GPa) and other metals. This provides high rigidity and dimensional stability of sheet, foil, strip, and wire… However, with increasing temperature, the elastic modulus of rhenium decreases, and at temperatures above 1000°C, rhenium has no longer an advantage on tungsten.

At room temperature, rhenium combines high strength and ductility: ultimate tensile strength (UTS) of wire 1.27-1.6 mm diameter is about 1200 MPa with relative elongation (EL) = 25%. Single-crystal rhenium produced by ZEBM has UTS = 500 MPa and EL = 100%. An addition of 10 atomic percent Mo increases UTS to 850 MPa and decreases EL to 60%. The larger the atomic percentage of Mo and W, the more χ phase is formed, which decreases both strength and ductility of rhenium. Figure 2 presents the UTS of rhenium compared with other refractory metals.

At high temperatures (up to 2400-2700 °C), rhenium surpasses both bcc refractory metals from group VA and group VIA and the fcc and hcp refractory noble metals Ir, Rh, Os, and Ru in short term strength. Thus, at 1600 and 2000 K, rhenium has UTS of 360 and 200 MPa, respectively. The UTS values of tungsten, molybdenum, tantalum, and niobium at 1600°C do not exceed 200, 180, 100, and 90 MPa, respectively. The long-term (10 h) strength is also substantially higher than those of unalloyed W, Mo, Nb, and Ta at least up to 3000 K.

In strength, pure rhenium ranks above pure forms of other refractory metals (cf. Figure 2) but below modern bcc refractory alloys including the W and Mo alloys containing rhenium, carbides, or oxides at temperatures up to 2000-2400 K. However at

temperatures above $0.7T_m$, the contribution of the solid-solution strengthening both in rhenium alloys and in the alternative and competitive tungsten alloys is virtually absent and the contribution of dispersion hardening abruptly decreases. Rhenium exhibits a sharp increase in high-temperature ductility at about 2000°C, which is the temperature at the completion of recrystallization, but not at the starting recrystallization temperature as the majority of bcc refractory metals exhibit. A high ductility is maintained on the entire range of temperature as seen previously. This causes rhenium to be insensitive to thermal shock and to thermal cycling. Thruster nozzles produced from rhenium have undergone 100,000 thermal fatigue cycles from room temperature to over 2500 K without failing. Rhenium with high concentrations of interstitial impurities retains the ductility reserve upon operating in nitrogen-, oxygen-, and carbon-containing environments [6].

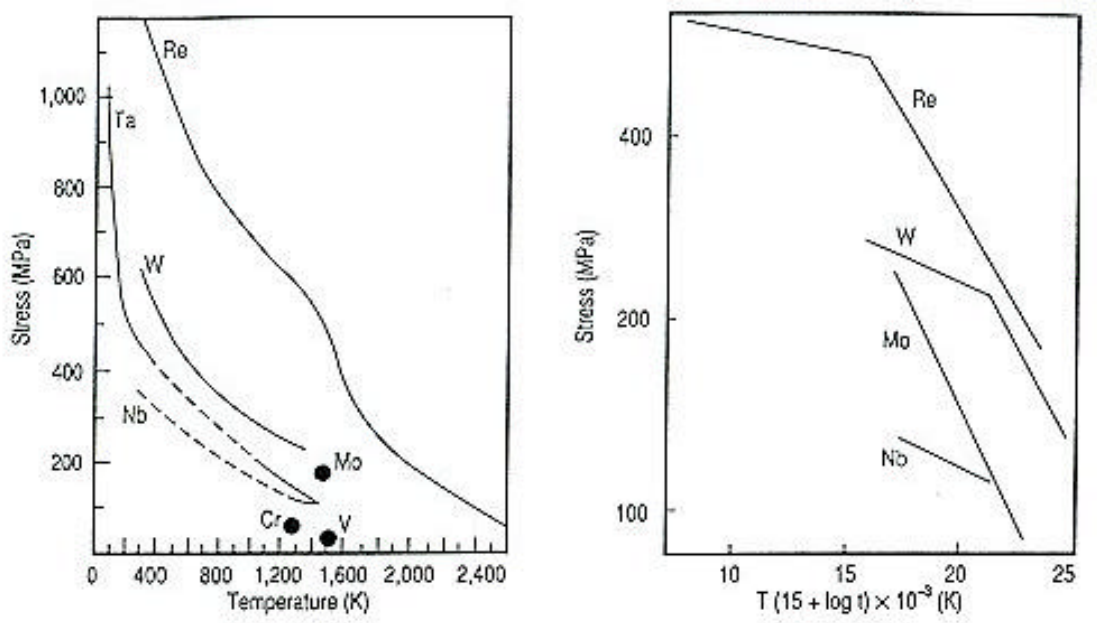

Figure 2: Ultimate Tensile Strength (UTS) of refractory metals (left). Creep-Rupture Strength of refractory metals (right) (from Bryskin B. D. 1992)

Rhenium as an Alloying Element

The effect of adding rhenium to other refractory metals on their high-temperature properties has been studied. Rhenium decreases melting temperatures of the more refractory transition metals of groups III and IV (Sc, Y, Nb, Ta, W, and Mo), and increases the melting point of the more fusible metals of the period I in the Periodic table (Ti, V, Cr, Mn, Fe, Co, and Ni) and of all VIII-group noble metals including the most refractory ones (Rh, Ru, Os, Ir, Pd, Pt).

Diffusion of rhenium in refractory metals occurs at rates as low as the rate of rhenium self-diffusion. Alloying of bcc refractory metals W and Mo with rhenium up to 20-30 atomic percents increases the diffusion rate by one to two orders of magnitude, which correlates to the melting temperature decreasing in this alloy due to rhenium additions. The inverse is to be expected for more fusible metals whose melting point is increased due to alloying with rhenium.

The effect of rhenium on the ductility of cold-brittle bcc metals of group VIA (W, Mo, and Cr) is unique. As mentioned previously, the “rhenium effect” consists of lowering the ductile-to-brittle transition temperature to below room temperature, which allows better ductilitity and workability. It also gives better allied characteristics such as an improvement of the weldability, and a decrease in the tendency of splitting and cracking in longitudinal and sections. It also increases strength at low and high temperatures. The explanations for this “rhenium effect” have been (and still are) the subject of several research projects. These include the increase in the state density of Fermi surface, the increase in the solubility of interstitial impurities in solid solution and the decrease in their tendency to segregate at lattice defects. As for the elements of group VA, low levels of rhenium additions to niobium and tantalum result in a dramatic loss of

low temperature ductility, which is opposite to what is observed when rhenium is added to metals of group VIA, in other words the so called “Rhenium Ductilizing Effect” is not observed with elements of group VA.

The effect of rhenium on strain hardening of metals is known as the “Rhenium effect-2”. Bcc metals (Nb, Mo, Ta, W) or fcc metals (Ni) are usually strengthened upon cold working but only weakly. However, addition of rhenium increases their ability to strain-harden. This effect of rhenium on strain hardening was used for the design of elastic elements with the ultimate tensile strength up to 5000-7000 MPa [4].

Interactions of Rhenium with Other Elements

To date, the interaction of rhenium with 64 elements is known. More than 100 complete or partial binary and ternary phase diagrams have been constructed that were used to establish some features of the interaction of rhenium with other elements.

The maximum solubility of metals in rhenium is determined by their crystal lattice, their difference in atomic radii (ΔR) and electronegativities (ΔE). The solubility of nonisomorphic metals in hcp rhenium is generally low, since the ΔE and ΔR values are higher. For the same values of ΔE and ΔR, solubility of fcc metals in rhenium is significantly higher than that of bcc metals. The solubilities of fcc and bcc metals in rhenium sharply decrease as ΔR increases above 5% and ΔE increases above 0.1.

The intermetallic compounds of rhenium with transition metals are mainly of three types: λ, σ, and χ phases. The type of intermetallic compound depends on dimensional (R_{metal}/R_{Re}), the electrochemical factors determined by the position in the periodic table, and by the electronic structure of the metal. The stability of the Laves phases is maximum in systems involving electropositive metal of group-III characterized

by R_{metal}/R_{Re} = 1.25-1.37; typical values of this ratio for λ phases are in the range: 1.1-1.5. As the R_{metal}/R_{Re} ratio decreases, χ phase (involving group-III metals such as Sc) and σ phase (involving group-IV metals such as Zr and Hf) appear in the systems in addition to the λ phase. The stability of the Laves phase is less for R_{metal}/R_{Re} ratios less than 1.1; the χ phase looses stability as R_{metal}/R_{Re} decreases to about 1.0. This phase is most stable when the rhenium intermetallic system involves metallic elements from group IV and group V, and the σ phase is most stable in systems with the group-VI elements. The σ phases form at temperatures above 2350 °C and exist in a wide range of concentrations. The σ phases are less stable when they involve elements of groups V, VII, and VIII, which they actually decompose by eutectoid reactions. All intermetallic compounds in the systems of rhenium form by peritectic reactions, except the χ phases in the systems involving metals of group VIA. In the systems with W or Mo, the χ phases form by peritectoid reactions, and the χ phase stability is lost when the other metal has a different electronic structure or that the R_{metal}/R_{Re} is not adequate.

Chemical Properties

Chemically, rhenium behaves as a half-noble metal, but its behavior depends on its state of division. The massive metal remains unchanged in the air, while a fine powder may be pyrophoric. When heated in oxygen, Re_2O_7 forms; dry chlorine acts on rhenium below 100 °C to give volatile chlorides; bromine does so less readily, and iodine not at all. Sulphur converts it into the disulphide ReS_2; nitrogen has no action at any temperature up to 2000 °C. Metallic rhenium has a good resistance to sulfuric acid and a very high corrosion resistance to resistance to hydrochloric acid. Actually, air-free water,

either alone, or when it contains HF, HCl, HBr, H_2SO_4, KOH, or ammonia, has practically no effect on the metal. But rhenium metal is readily attacked by oxygen, especially in the presence of concentrated acids, and oxidizing chemical substances like HNO_3, H_2O_2, or chlorine water.

Under conventional conditions, rhenium does not form stable carbides and nitrides. If rhenium is put in a heated methane atmosphere, it begins to decompose at 800 °C, and the separated carbon dissolves in the metal up to 0.9 %, but no carbides form at temperatures up to 2000 °C. Metallic rhenium powder is however said to form a carbide when heated in carbon monoxide above 500 °C (Re_4C_3). Although carbon diffusion into rhenium causes some solid solution hardening, no catastrophic embrittlement occurs as when carbide forms in tungsten, molybdenum and other refractory metals. Therefore rhenium could be used in contact with graphite and carbon composites. However, the solubility of carbon in rhenium results in a eutectic melting point of 2773 K with approximately 0.85 wt % of carbon.

The rhenium halides are volatile and their compounds decompose easily, which makes their use for the production of rhenium and its alloys with W and Mo by CVD method possible. Rhenium also interacts with alkalis (especially, in the presence of potassium ferrocianide).

Rhenium can have valences from –1 to +7 depending on the compound it is in. The most stable rhenium oxide Re_2O_7 forms at temperature above 160 °C, melts at 279 °C and sublimates without decomposition at temperatures above 400 °C. Re_2O_7 has a good electrical conductivity. This provides good contact resistance stability under oxidizing environments. Rhenium is oxidized in steam forming Re_2O_7, but its evaporation and transfer of Re upon “water cycle” in electronic devices are substantially

smaller than those of tungsten. At higher temperatures in oxygen-containing atmospheres, the Ir coating helps protect it from oxidation.

The main rhenium oxides are rhenium heptoxide Re_2O_7, rhenium trioxide ReO_3, rhenium dioxide ReO_2, and rhenium sesquioxide Re_2O_3. The greater the valence of the metallic rhenium involved, the more stable the oxide is.

Re_2O_7 is obtained when the metal is heated in oxygen to a temperature about 150 °C; it is also formed when an aqueous solution of perrhenic acid $HreO_4$ is evaporated to dryness, and it is always produced whenever rhenium compounds are ignited in oxygen. Re_2O_7 exists in two forms white and yellow. The white form is not very well understood. It is formed by the direct oxidation of rhenium or its dioxide, when a cold stream of oxygen gas gets in contact with the hot metal or oxide. At 150 °C, the white form changes to the yellow form without any loss of oxygen, which implies the two forms must be isomeric. The yellow form of Re_2O_7 is the usual form; it darkens when heated, however at –80 °C it is colorless. Solid Re_2O_7 melts at 304 °C and boils at 350 °C. Its vapor is colorless, stable, and monomeric at least up to 520 °C. It is easily soluble in water in which it is reversibly hydrated. Hydrogen reduces Re_2O_7 to its blue-black ReO_2 at 300 °C, and to rhenium metal at 500 °C.

ReO_3 is obtained by heating rhenium with the heptoxide at temperatures about 200-250 °C, or by burning the metal in a slight atmosphere containing oxygen. The powder formed can have any color from dark-blue to copper color according to its state of division. Its crystalline structure is similar to that of WO_3; it is not attacked by water, or by hydrochloric acid (even hot). If it is heated alone *in vacuo* to 400 °C it is converted to rhenium dioxide and heptoxide.

ReO_2 is produced by heating rhenium metal in a low supply of oxygen or by reducing the higher rhenium oxides with hydrogen. Anhydrous rhenium dioxide is a black powder that absorbs greatly solutes and gases. Although it is very stable in oxygen-free conditions, if it is heated to high temperatures it is converted in vacuo into a mixture of metallic rhenium and rhenium heptoxide. If heated in oxygen, rhenium dioxide is converted to heptoxide.

Rhenium sesquioxide Re_2O_3 has only been prepared in an hydrate form that appears as a black precipitate when a solution of trivalent rhenium (like $ReCl_3$) is treated with alkali hydroxide. It is very easily oxidized by oxygen contact [13, 14].

Figure 3 shows the corrosion rate for some refractory metals, in air. It appears clearly that Re has very poor resistance to oxidation compared to other refractory metals, especially tungsten.

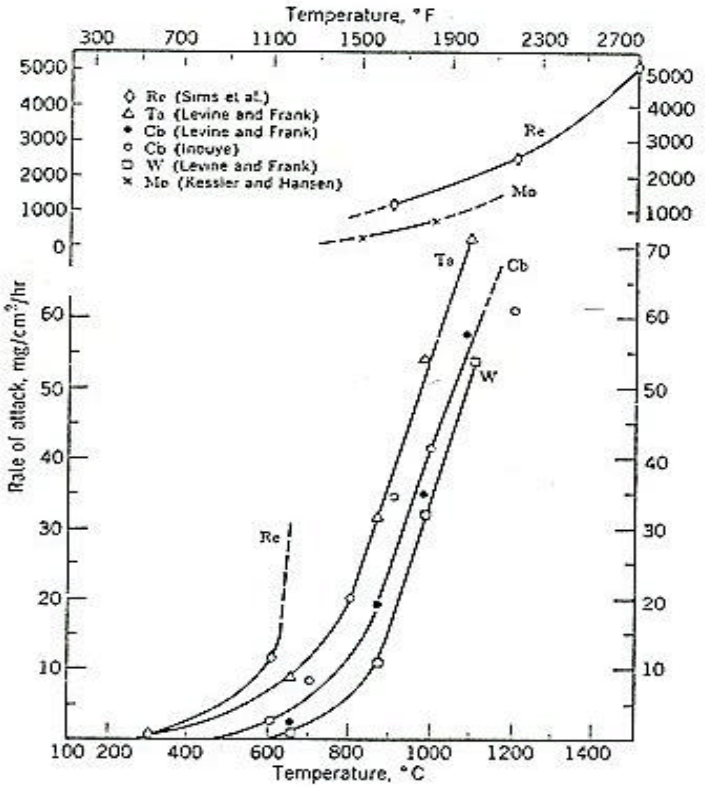

Figure 3: Rate of corrosion of refractory metals in air.

CHAPTER 3
THEORETICAL AND EXPERIMENTAL INVESTIGATIONS ON THE COMPATIBILITY BETWEEN URANIUM DIOXIDE AND RHENIUM.

Thermodynamic Considerations: Predictions Based on F*A*C*T code

When chemically reactive species are put together under certain conditions of pressure and temperature, chemical reactions can take place, and several different compounds may be formed, but out of all the possibilities, only the stable compounds will be part of the final composition, once chemical equilibrium is reached. Of all possible products, the most stable ones are those resulting from spontaneous reactions since the more spontaneous the reaction, the more likely the corresponding products are to form. Some reactions are spontaneous because they give off energy in the form of heat ($\Delta H < 0$). Others are spontaneous because they lead to an increase in the disorder of the system ($\Delta S > 0$). ΔH is the change in enthalpy (heat content of a substance) due to the reaction, and ΔS the change in entropy (the degree of disorder in a system). Therefore, calculations of ΔH and ΔS can be used to probe the driving force behind a particular reaction. However, it can happen that one of the potential driving forces behind a chemical reaction is favorable and the other is not. In that case, whether the reaction is likely to happen or not cannot be answered obviously. The Gibbs free energy function was thus created in order to solve the problem. It actually reflects the balance between the two driving forces. The Gibbs free energy of a system at any moment in time is defined

as the enthalpy of the system minus the product of the temperature times the entropy of the system:

$$G=H-TS$$

The change in the Gibbs free energy of the system that occurs during a reaction is therefore equal to the change in the enthalpy of the system minus the change in the product of the temperature times the entropy of the system.

$$\Delta G = \Delta H - \Delta(TS),$$

which becomes:

$$\Delta G = \Delta H - T\Delta S,$$

when the reaction is run at constant temperature. When ΔG is negative the reaction is spontaneous process and is giving off energy. In other words, the lower ΔG, the higher the probability of occurrence of the reaction, and the more stable the chemical compound produced is. When ΔG is positive the reaction is not spontaneous since the reaction would need energy from a catalyst for it to take place, therefore the corresponding products of the reaction are unlikely to be formed; they are not considered as stable. The values for G, S, and H (which are all state functions) may be found in data tables at any set of temperature and pressure values for any element or compound for which data is available. Thus, the value of ΔG for a reaction, under specific temperature and pressure values can be calculated. And the probability of formation of a specific compound can be evaluated. At the specified temperature and pressure, the most stable product will be the one resulting from the reaction with the lowest change in Gibbs free energy (ΔG).

Based on this principle, the numerical code F*A*C*T (and more particularly "EQUILIB", a program that is part of the code) is used to determine the equilibrium composition of a system given the reactants, the final conditions (temperature and pressure). The program actually proceeds through a search of all possible product compounds found in an internal database. And after calculation of the corresponding G values, the output reprints the reactants as well as the predicted most stable quantities of the possible products initially selected in the database mentioned previously. Therefore, it can be seen whether a product is likely to form or not, at the specified final temperature and pressure, given the input reactants.

The code was used in order to determine the expected composition of a system initially composed of rhenium and uranium dioxide. This actually gives the same results as those that one would obtain by inputting uranium, dioxygen, and rhenium as the reactants, since the list of possible products that the program selects in its database is the same in both cases, which means that the code selects the possible products according to the elemental initial composition. The runs were done for different temperatures ranging from 2000 K to 3000K, for a final pressure of 1 atmosphere. The results for the runs of interest are given below (Tables 1, 2 and 3).

Before making any conclusions based on these runs, it is important to remind the limitations of the code that supposes ideal conditions and whose database is certainly not exhaustive; for instance, rhenium sesquioxide Re_2O_3 was not included in the internal library of the code. Another limitation of the EQUILIB code is that it ignores the kinetics of the reaction. It actually gives the final composition of the system, assuming the equilibrium is reached and does not take into account the fact that the equilibrium may be

long to reach; and it can happen that the kinetics associated with the formation of a compound that appears to be stable (from a thermodynamic point of view) is so slow that it may not be observed during the real experiment. Those are the two main limitations of the code that one should keep in mind before interpreting any result.

Table 1: Results obtained with the F*A*C*T code for the Re/O_2 system at different high temperatures.

Reactants and their initial quantities		Re (1 mole), O_2 (1 mole)	
Possible products looked at by F*A*C*T		O, O_2, O_3, Re, (gas and solid), Re_2O_7 (gas and solid), ReO_2, ReO_3	
Final pressure and temperature	1 atm, 2400 K	1 atm, 2600K	1 atm, 3000K
Product formed and their equilibrium concentration (the activity of the phase formed is given)	0.28977 mol of (0.98064 Re_2O_7 + 0.18197E-01 O_2 + 0.11624E-02 O + 0.56857E-07 Re + 0.54939E-08 O_3) (ideal gas) + 0.43168 mol Re (solid)	0.30079 mol of (0.93099 Re_2O_7 + 0.63196E-01 O_2 + 0.58142E-02 O + 0.10113E-07 Re + 0.62505E-08 O_3) (ideal gas) + 0.43993 mol Re (solid)	0.44308 mol of (0.51719 Re_2O_7 + 0.41070E-01 O_2 + 0.72108E-02 O + 0.98402E-07 Re + 0.25548E-08 O_3) (ideal gas) + 0.54169 mol Re (solid)

Table 2: Results obtained with the F*A*C*T code for the rhenium-oxygen system with excess oxygen, at different high temperatures.

Reactants and their initial quantities	Re (1 mole), O (1 mole), 02 (1 mole)
Possible products looked at by F*A*C*T	O, O_2, O_3, Re, (gas and solid), Re_2O_7 (gas and solid), ReO_2, ReO_3
500 K, 1000 K, 1500 K	1.0000 mol ReO_3
1800 K	0.42860 mol of (0.99991 Re_2O_7+ 0.84269E-04 O_2 + 0.11097E-05 O + 0.15140E-13 O_3 + 0.19531E-14 Re (ideal gas) + 0.14288 mol Re (solid)
2000 K	0.42880 mol of (0.99927 Re_2O_7 + 0.71649E-03 O_2 + 0.17792E-04 O + 0.99303E-12 O_3 + 0.30445E-12 Re) (ideal gas) + 0.14303 mol Re (solid)
2500 K, 2800 K, 3100 K	0.42857 mol Re_2O_7 (liquid) + 0.14286 mol Re (solid)
3500 K	1.8431 mol (0.61362 O_2 + 0.38395 O + 0.23620E-02 Re_2O_7 + 0.64235E-04 Re + 0.10778E-05 O3) (ideal gas) + 0.99118 mol Re (liquid)

Table 3: Results obtained with the F*A*C*T code for the Re/UO2 system at different high temperatures.

Reactants and their initial quantities	Re (1 mol), UO_2	
Possible products looked at by F*A*C*T	O, O_2, O_3, Re, ReO_3 (solid), ReO_2, Re_2O_7, U, UO, UO_2, UO_3, U_4O_9, U_3O_8	
Final pressure and temperature	1 atm, 2000 K, 2200 K, 2400 K, 2600 K, 2800 K, 3000 K	1 atm, 4000 K
Product formed and their equilibrium concentration (the activity of the phase formed is given)	1.00000 mol Re (a=1.00000) 1.00000 mol UO_2 (a=1.00000)	1.0369 mol of (0.80387 UO2 + 0.96479E-01 UO + 0.63288E-01 UO3 + 0.33783E-01 O + 0.12402E-02 Re + 0.81685E-03 U + 0.52077E-03 O2 + 0.49788E-10 O3 + 0.17468E-15 Re2O7) (ideal gas) + 0.99871 mol Re (liquid)

In the case where the system is initially composed of 1 mole of rhenium and 1 mole of uranium dioxide, the only rhenium oxide that forms in the temperature range of interest is rhenium heptoxide (Table 1). The code was also run for an initial composition of 1 mole of Re with 1 mole of O_2 and 1 mole of O in order to simulate the case where rhenium is in excess of oxygen. The results are given in Table 2. The oxidation of rhenium is quantitatively more important since less rhenium is left unreacted in a solid phase. For the lowest temperatures, ReO_3 is the only stable compound appearing in the equilibrium composition. This is because rhenium trioxide has a lower enthalpy of formation than that of rhenium heptoxide at low temperatures. Actually, the use of REACTION (an other code included in F*A*C*T) showed that even rhenium dioxide is more stable than Re_2O_7 at low temperature from a thermodynamic standpoint (? G values), but it is less stable than ReO_3, which explains why it does not appear in the final composition. Between 1600 K and 1800 K, a change occurs: the enthalpy of formation for high temperatures is less for Re_2O_7; therefore, rhenium heptoxide becomes the most stable rhenium oxide and thus it is the only oxide that appears in the equilibrium composition. For temperatures higher than the melting point of rhenium, 3500k for instance, very little rhenium is found in the form of oxide; 99.8% of the initial rhenium is found in a pure liquid phase (less reactive).

Therefore, the results show that in the range of temperatures of interest (2000 K-3000 K), rhenium in presence of oxygen does form rhenium oxides in a gas phase (Table1 and Table 2). However, when uranium is present in the system, rhenium does not form any stable oxide because uranium dioxide has a much lower Gibbs free energy than any of the possible rhenium oxides (Table 3). Therefore UO_2 is the most stable phase; It

is not expected to interact with Re. At 3000 K, the code predicts that uranium dioxide remains totally stable, which is doubtful, since it should start dissociate as the sublimation temperature is approached. For an ultrahigh temperature such as 4000K, most of the uranium dioxide is supposed to volatilize, some UO and UO_3 are also supposed to form; rhenium is mainly unreacted (in a liquid form), the rest of it is found in a vapor phase; extremely little quantity of Re_2O_7 is found in the final atmosphere. Rhenium appears to be less oxidable in a liquid form. However, the most important part of these runs is that for the temperature range [2000 K-3000 K], rhenium and uranium dioxide are expected to remain unreacted. Those runs are to be taken as a complement to a necessary experimental investigation that needs to be done. This experimental investigation is described below.

Experimental Work

Principle of the Method

Experimentally, the compatibility of rhenium (Re) with uranium dioxide (UO2) was determined mainly by comparing the spectrums obtained from the X-Ray powder Diffraction (XRD) analysis of a mixture of Re and UO_2 powders before and after it was sintered for ten hours at 2500 K. The XRD pattern of a sample gives its phase/elemental composition. Therefore, by comparing the XRD spectra of the initial mixture and the sintered mixture, it was possible to determine whether a new compound or more generally a new phase were formed during the sintering. The compatibility of Re with UO_2 could be assessed only if the spectra of the pre-sintering and post-sintering samples have similar peak characteristics. A visual inspection of the samples using Back-scattered

Electron Microscopy (BSE) was also done to complement the conclusions that could be derived from the XRD analysis.

Materials/Protocol

The rhenium powder was 99.999% pure and the urania powder, 99.98% pure. The average sizes of the powders were respectively –50 mesh (<300 μm) and –22 mesh (<800 μm). Since the size of the rhenium powder particles was larger than the size of the urania particles, the proportion of urania particles had to be larger in order to enhance the surface contact of the UO_2 grains with the Re ones. For each sample, about 9 grams of urania were mixed to about 5 grams of rhenium. Each mixture was mixed for one day on a rotary tumbler in order to obtain a very homogeneous mixture. A picture of the tumbler is shown in Figure 4.

Figure 4: Rotary tumbler used to mix the Re powder with the UO_2 powder.

A small sample of this mixture was submitted to x-ray powder diffraction analysis. The rest of the mixture was pressed in a tungsten crucible with special care because of the extreme brittleness of tungsten. Indeed, high-pressure pressing would automatically result in cracks in the crucible wall, enhancing the possibilities of leakage. The samples were sintered in a 20 kW, 450 kHz induction heating furnace. A picture of the furnace chamber as well as a picture of the inside coil are shown in figures 5 and 6.

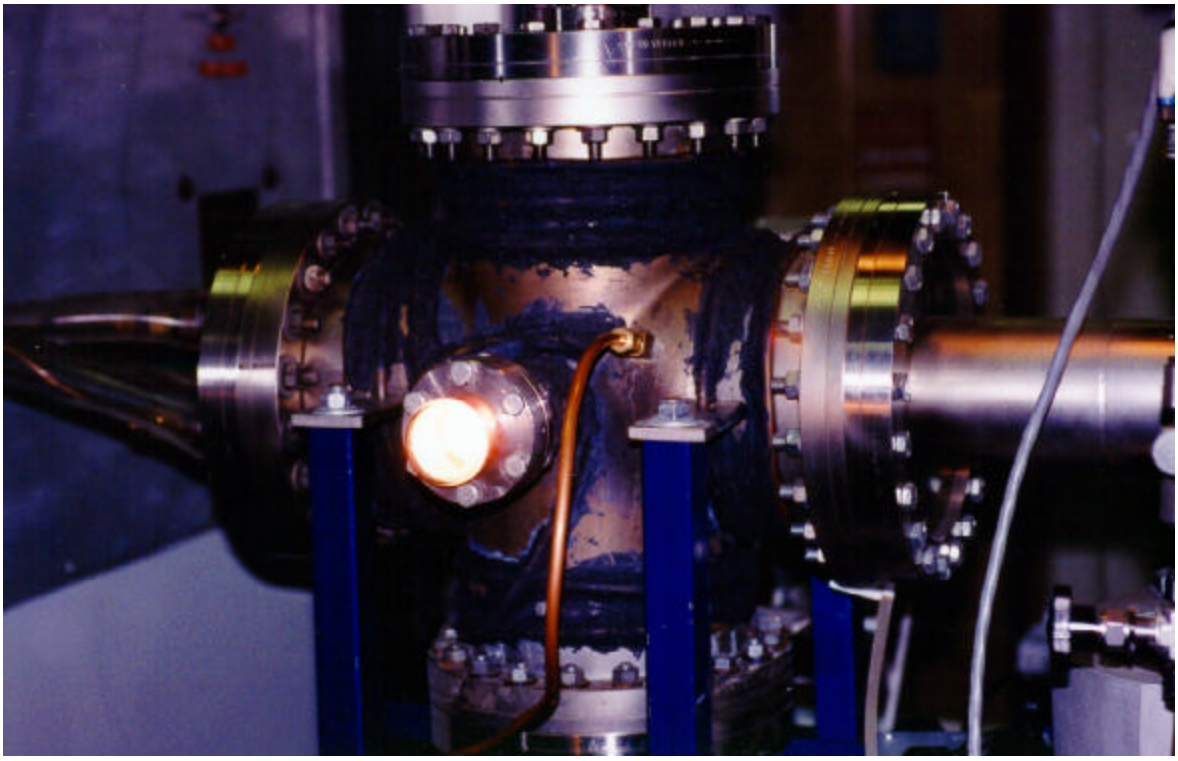

Figure 5: Induction-furnace chamber used for sintering the samples.

After removal from the crucible, each sample was sectioned using a slow-speed wafering saw. Part of the sample was mounted in epoxy resin and polished through 0.5 μm using diamond paste giving an individual section that could be examined using a Back-scattered electron microscope (BSE) equipped with energy dispersive x-ray

spectroscopy (EDS). The remaining of the sample was crushed into a fine powder that was subjected to phase analysis with an x-ray powder diffraction (XRD) device using CuK_{α} radiation. This analytical work was done using the available equipment of the Major Analytical Instrumentation Center (MAIC), one of the Materials Science and Engineering centers of the University of Florida. The principles of the analytical methods used are developed in the appendix attached to this work.

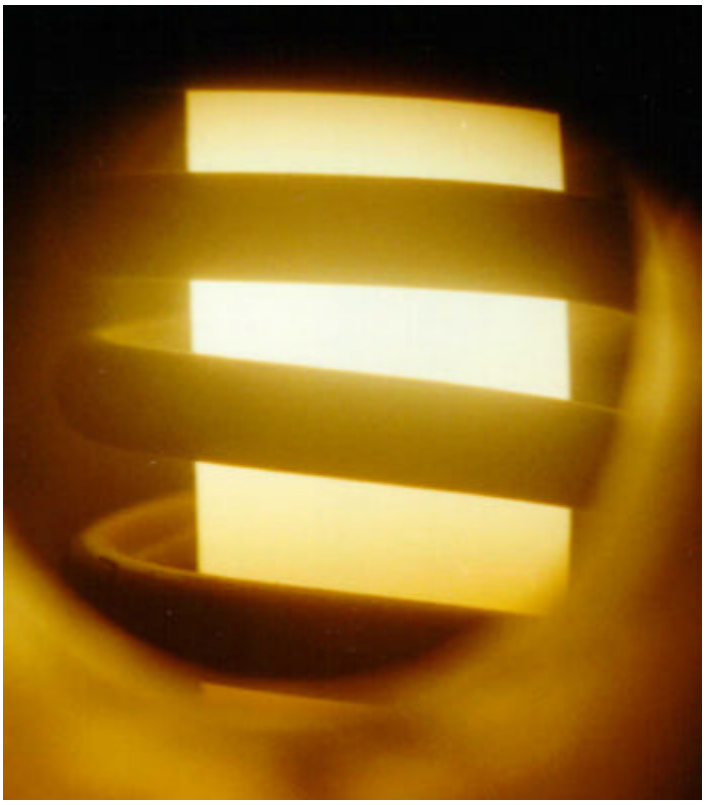

Figure 6: Inductive coil and heated susceptor radiating inside the furnace chamber.

Results

Sample 1

The sample was sintered for a total cumulative time of ten hours at 2500 K. The sintering process was then stopped due to an abnormal increase of the pressure inside the

furnace chamber, signaling a leak in the system. Once taken out of the furnace, the susceptor showed a long crack in the middle part, where the sample was located. This crack had have been initiated when the powder mixture was cold-pressed, due to the extreme brittleness of the tungsten crucible. Figure 7 shows the cracked susceptor with a protuberance built up on the outside part of the crack.

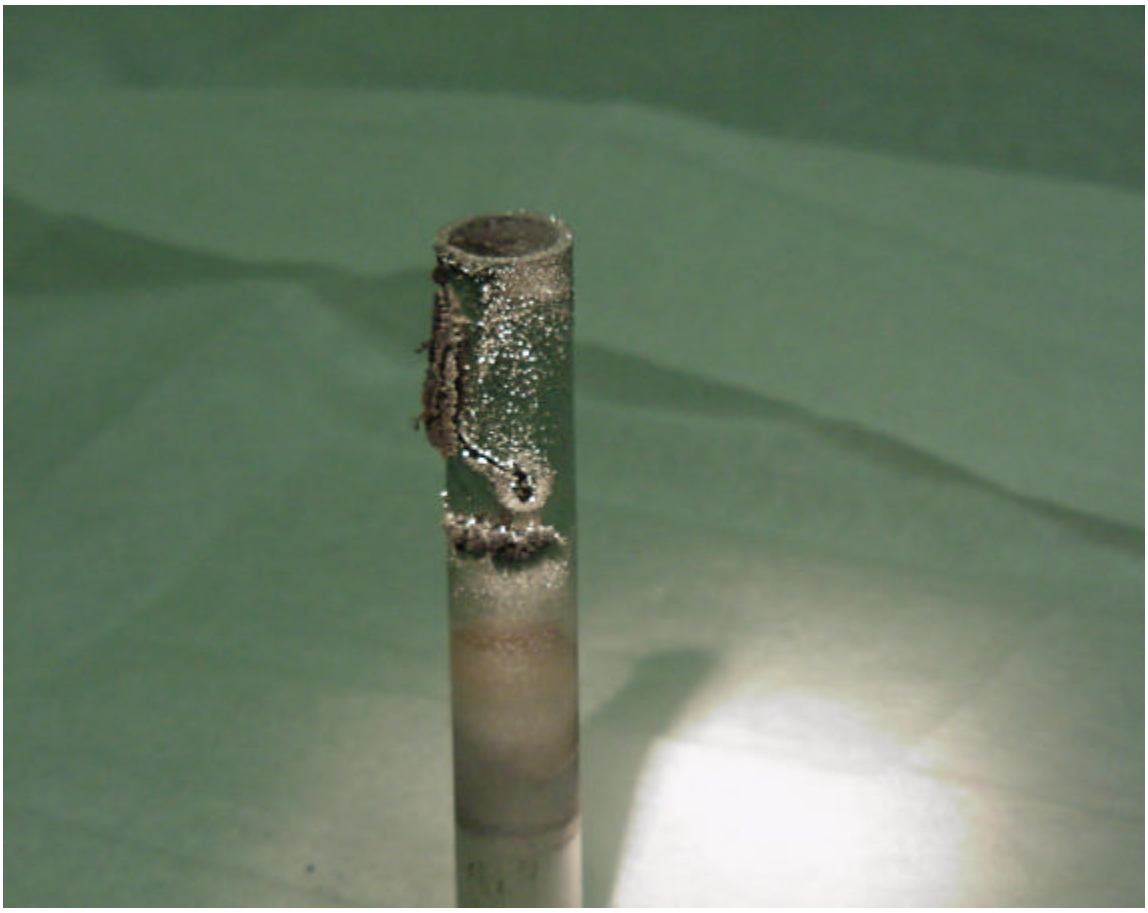

Figure 7: Tungsten susceptor after sintering Sample 1 at 2500 K for 10 hours.

The initial crack must have acted as a concentrator for magnetic lines generated by the inductive coil and therefore the induced heat and therefore temperature at the crack must have been much higher then in the rest of the crucible, higher then the tungsten

melting point, since the crucible obviously melted in this very precise region, increasing the width of the crack.

The crack actually allowed the mixture to migrate outside of the crucible. Little material was left inside the crucible in the region corresponding to the crack, which indicated that part of the initial mixture went through the crack. The sintered mixture left inside of the crack was x-ray analyzed and the pattern obtained is presented in Figure 9. This XRD pattern was compared to the XRD spectrum obtained from the x-ray powder analysis of the UO_2-Re mixture prior to sintering (Figure 8).

Two main comments must be made. First, none of the main peaks corresponding to any of the possible rhenium oxides or rhenium-uranium phases were observed. The only peaks present on the pattern were attributed to either rhenium or uranium dioxide. Second, the pattern was however different from that of the initial mixture prior to sintering: the relative heights of the rhenium and uranium dioxide peaks were not conserved. The intensity of the uranium dioxide peaks was somehow less important relatively to the intensity of the rhenium peaks, which was not the case prior to sintering. This shows that uranium dioxide migrated out through the crack more readily than rhenium that remained in larger quantities inside the cracked crucible.

The migration of the inside material through the crack gave rise to a growth on the outside wall. This protuberance of grayish color is shown in Figure 10. This protuberance was analyzed using x-ray powder diffraction analysis. The obtained pattern is shown in Figure 11.

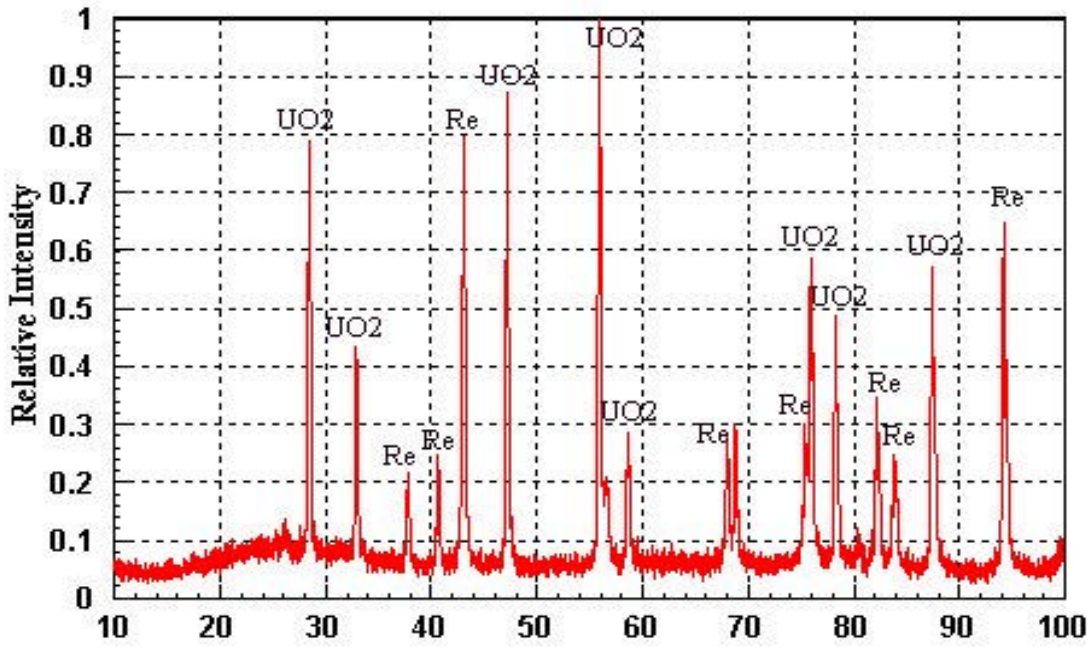

Figure 8: X-ray powder diffraction pattern of the pre-sintered of Re and UO_2 powders.

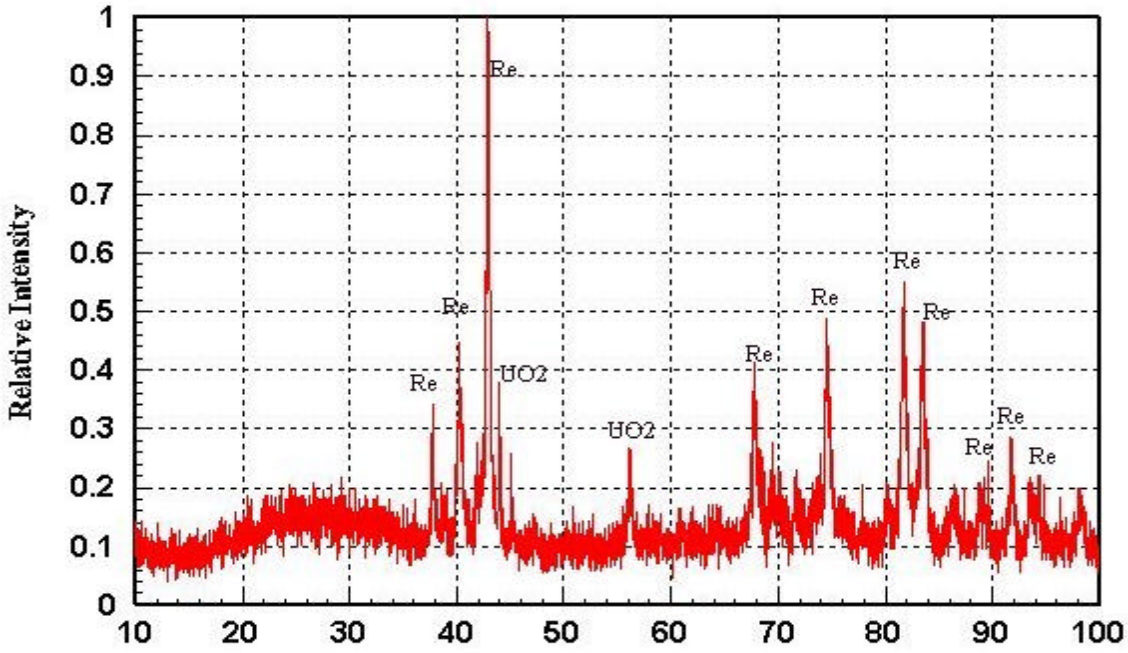

Figure 9: X-ray powder diffraction pattern of the sintered mixture of Re and UO_2 powders left inside the crack.

Note: All -ray powder diffraction patterns are given versus (2 theta).

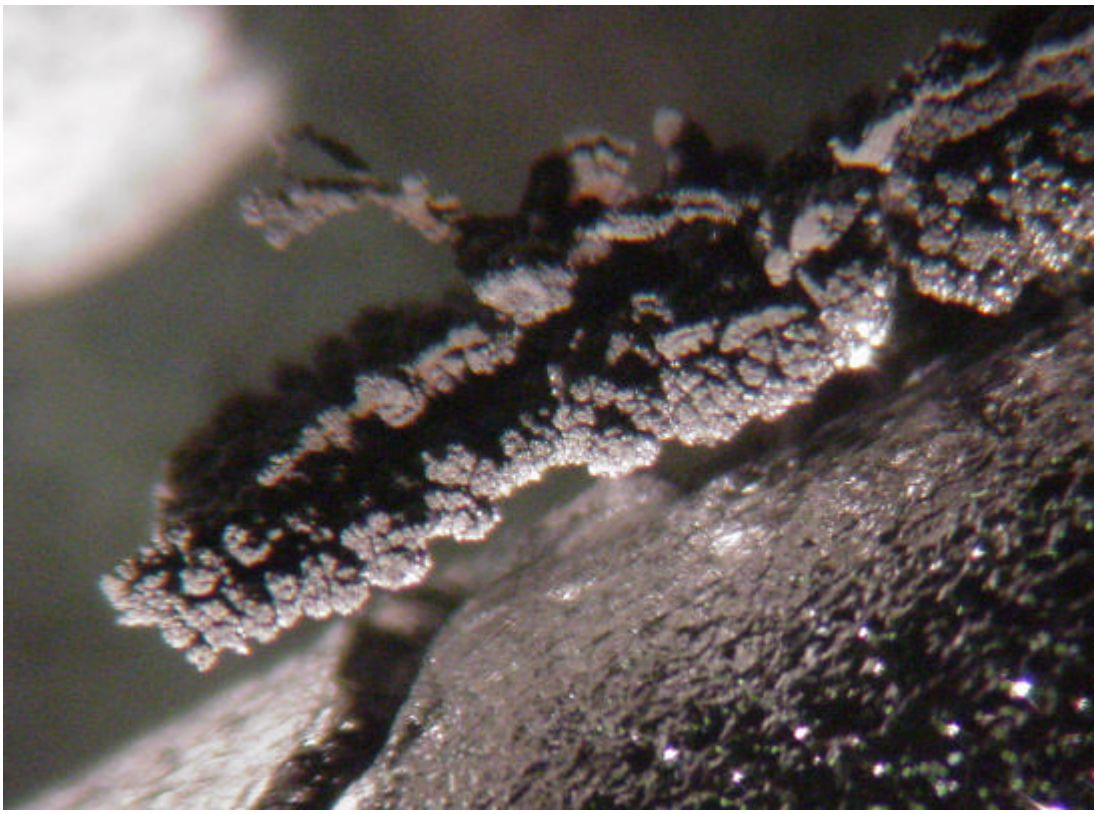

Figure 10: Growth outside of the crack.

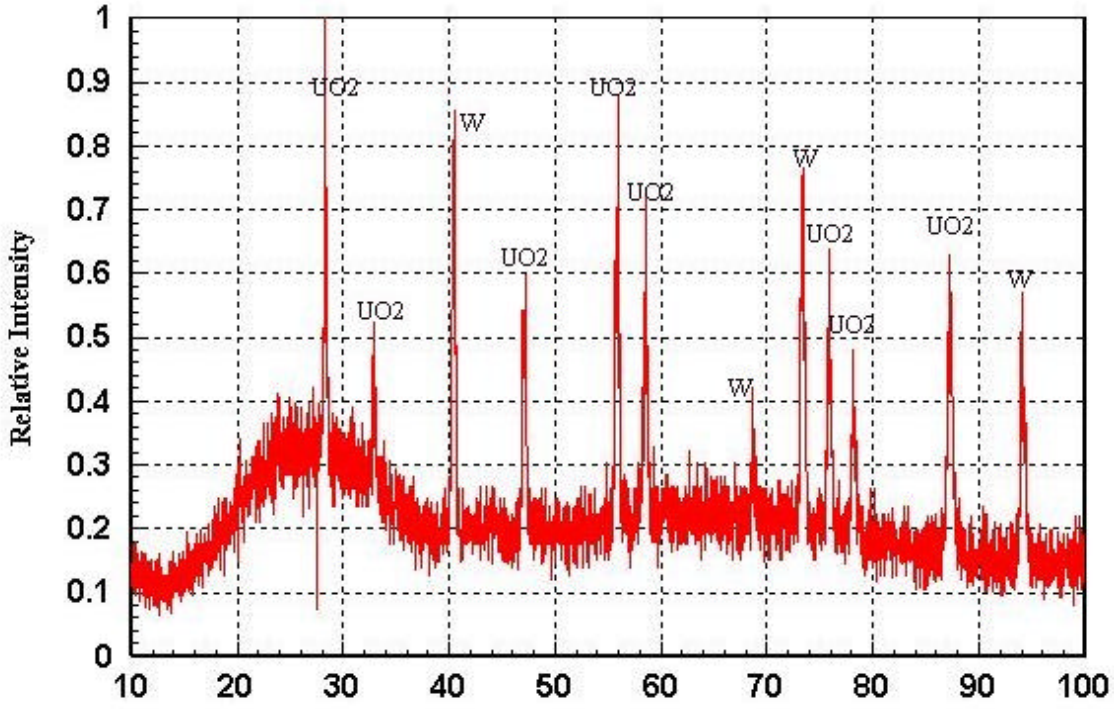

Figure 11: X-ray powder diffraction pattern of the growth outside the crucible.

Apparently, the outside growth was free of rhenium, but did contain tungsten (from the susceptor); if it contained some rhenium it must have been in very little quantities since none of characteristic peak of rhenium was observed in the pattern, which actually is consistent with the conclusions previously derived.

In the top region of the crucible, the inside mixture was clearly not altered like in the crack region. The x-ray analysis pattern obtained for that part of the sample is given in Figure 12. It is similar to the x-ray analysis pattern of the pre-sintered mixture. None of the main peaks corresponding to any of the possible rhenium oxides or rhenium-uranium phases were observed. However, some of the peaks did not have the expected height relatively to the other peaks of the series they belonged to. For instance, the peak referenced as 1, 2, and 3 were larger then expected. After investigation, they were identified as being also characteristic of tungsten. This showed that tungsten deposited on the top surface of the sample, which was open to the furnace chamber atmosphere.

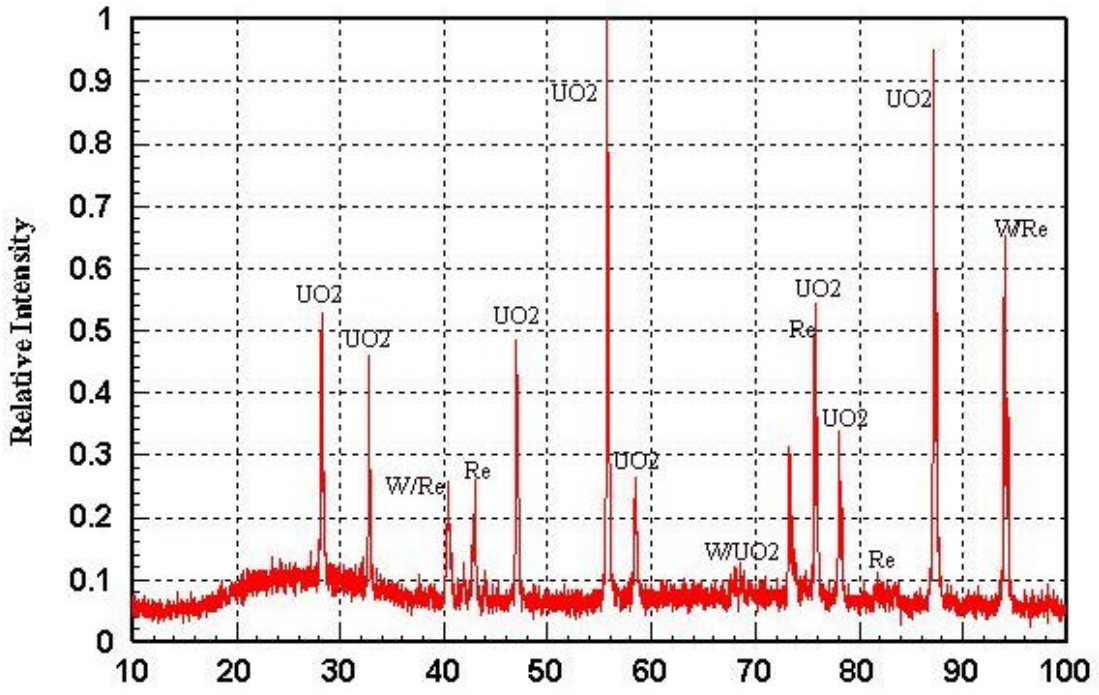

Figure 12: X-ray powder diffraction pattern of the top region of sample 1.

As a matter of fact, a dark-blue-black deposit was observed on the walls of the furnace, as well as on the copper coil (Figure 13). The deposit on the walls was x-ray analyzed in order to determine the compounds formed. Figure 14 gives the XRD spectrum obtained.

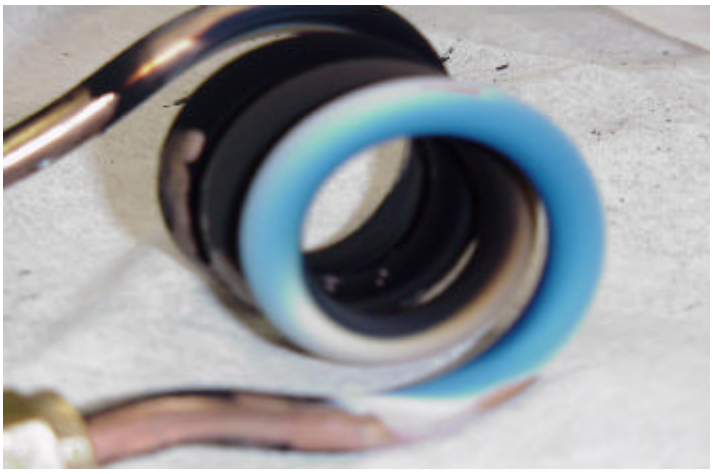

Figure 13: Dark deposit on the coil, after sintering the tungsten crucible the first time.

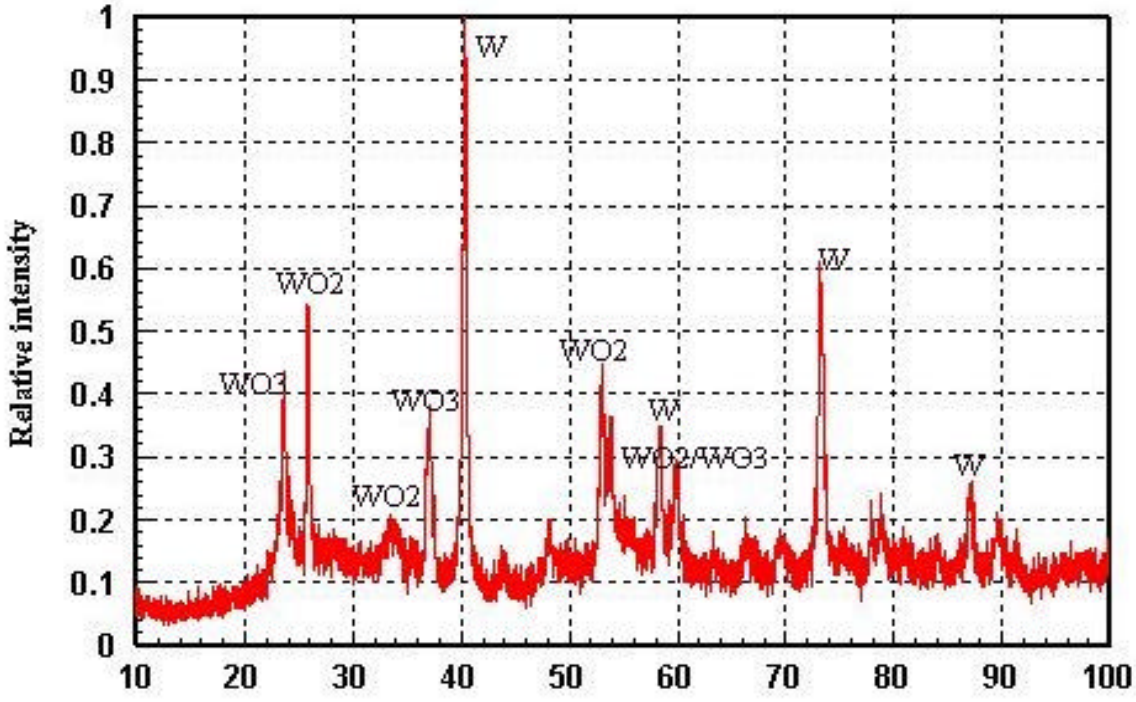

Figure 14. XRD pattern of the deposit found on the furnace chamber walls.

The spectrum clearly shows that this deposit on the walls of the chamber was tungsten and tungsten oxide. Special care was therefore further provided in order to keep the atmosphere in the chamber inert during the following runs; regular purges with argon would be operated.

Sample 2

Sample 2 was prepared using the same weight proportions as for sample 1. In order to avoid fissuring the tungsten crucible (like in the first experiment), the mixture of Re and UO_2 powders was not pressed; it was tamped. The sample was sintered for a total cumulative time of 10 hours at 2500 K. A picture of the baked crucible is given in Figure 15.

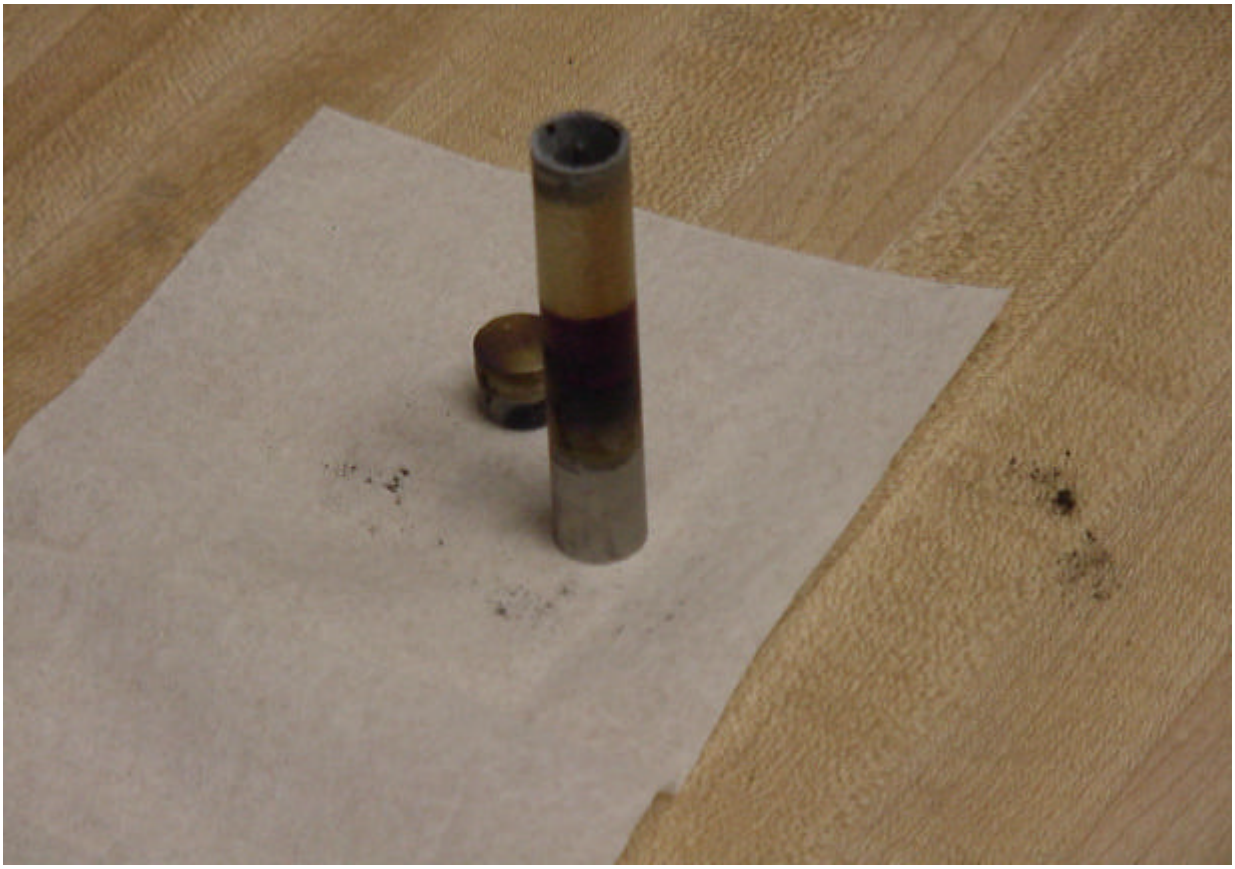

Figure 15: Tungsten susceptor after the sintering of sample 2.

After removal, the sample which was in a good condition in spite of the fact that there had been no cold-pressing of the initial mixture in order to avoid crack formation on the brittle tungsten crucible. The sample was sectioned using the wafering saw (as previously described in the protocol) and was submitted to x-ray analysis. The XRD pattern obtained for the bottom region is given below (Figure 17) as well as the pattern obtained from the pre-sintered initial mixture (Figure 16) for comparison.

The XRD pattern corresponding to the sintered sample was very similar to that of the pre-sintered mixture. Only peaks corresponding to Re and UO_2 were observed. None of the main peaks characteristic of pure uranium, Re-U phase, or any of the possible rhenium oxides were observed, which consolidated the conclusion that could already been derived from the results obtained for sample 1: rhenium did not chemically interact with uranium dioxide during the sintering process. Moreover the results were consistent for different sections of the sample analyzed. The XRD pattern corresponding to the middle part is shown in Figure 18.

Again, for this part, the sample was clearly composed only of rhenium and uranium dioxide, which is consistent with the conclusion previously derived. However, a series of new peaks appeared on this pattern, which was not present on the XRD pattern of the bottom region of the sample. These peaks actually were attributed to another phase of pure rhenium, which means that rhenium may give a new phase during sintering although it does not chemically react with uranium dioxide.

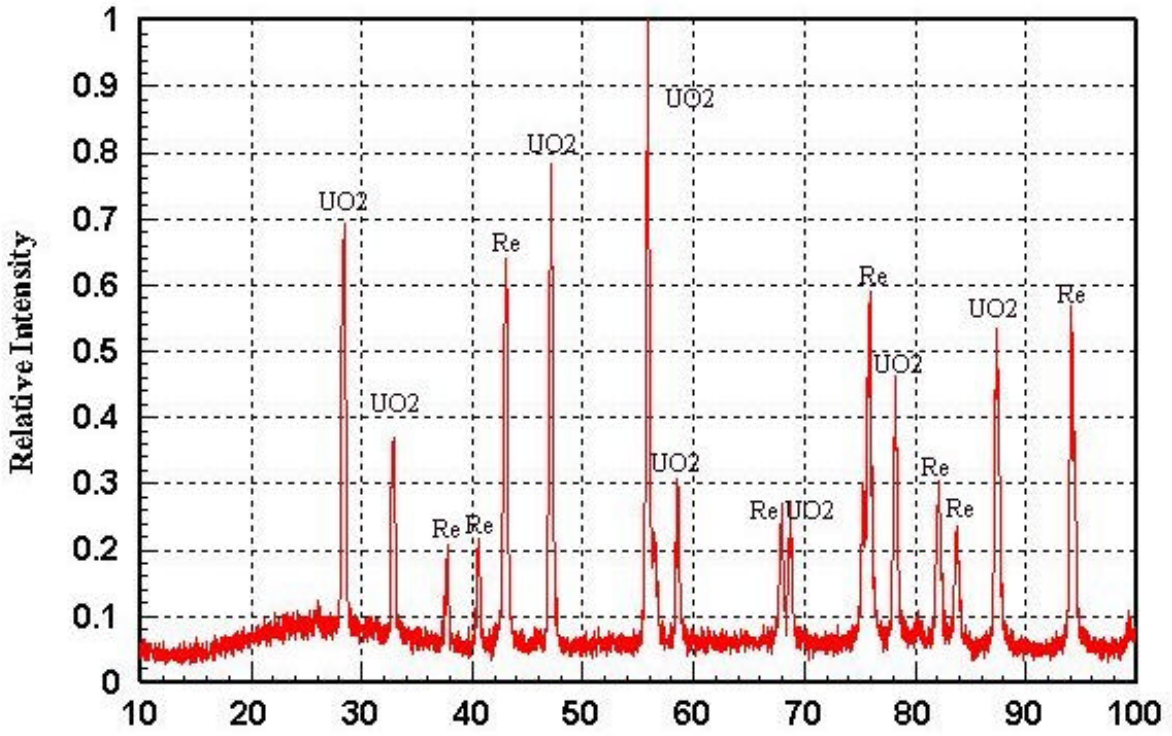

Figure 16: X-ray powder diffraction pattern of the pre-sintered mixture of UO_2 and Re powders.

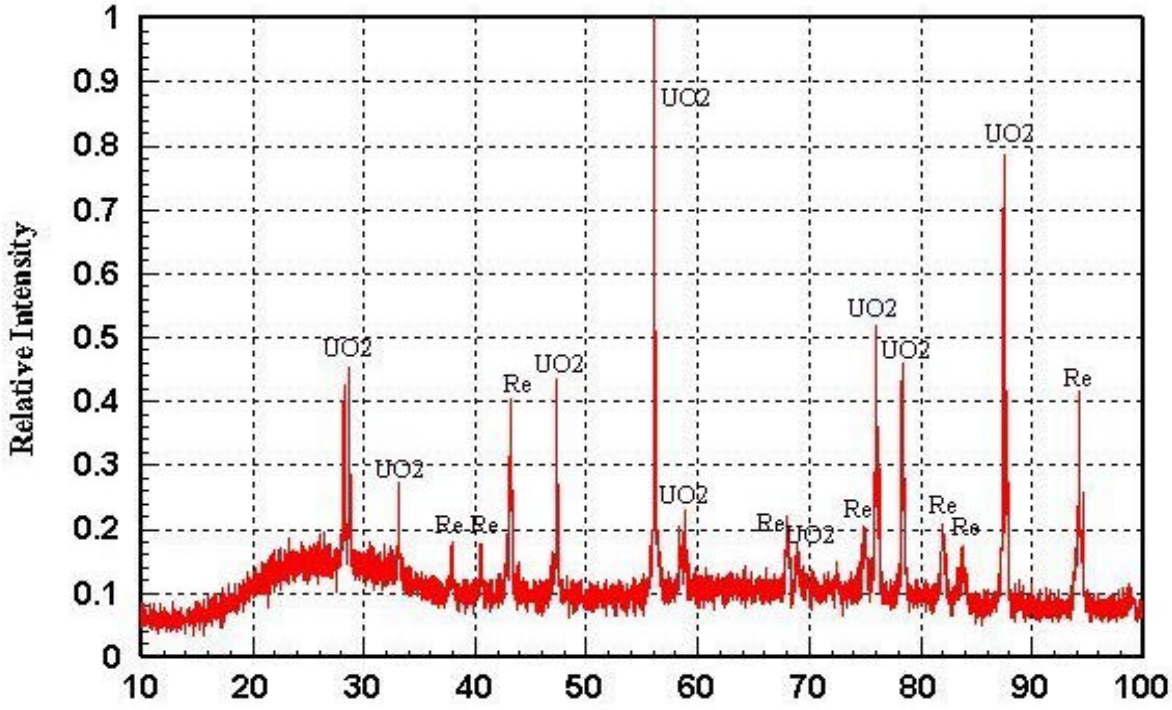

Figure 17: X-ray powder diffraction pattern of the bottom region of the sample.

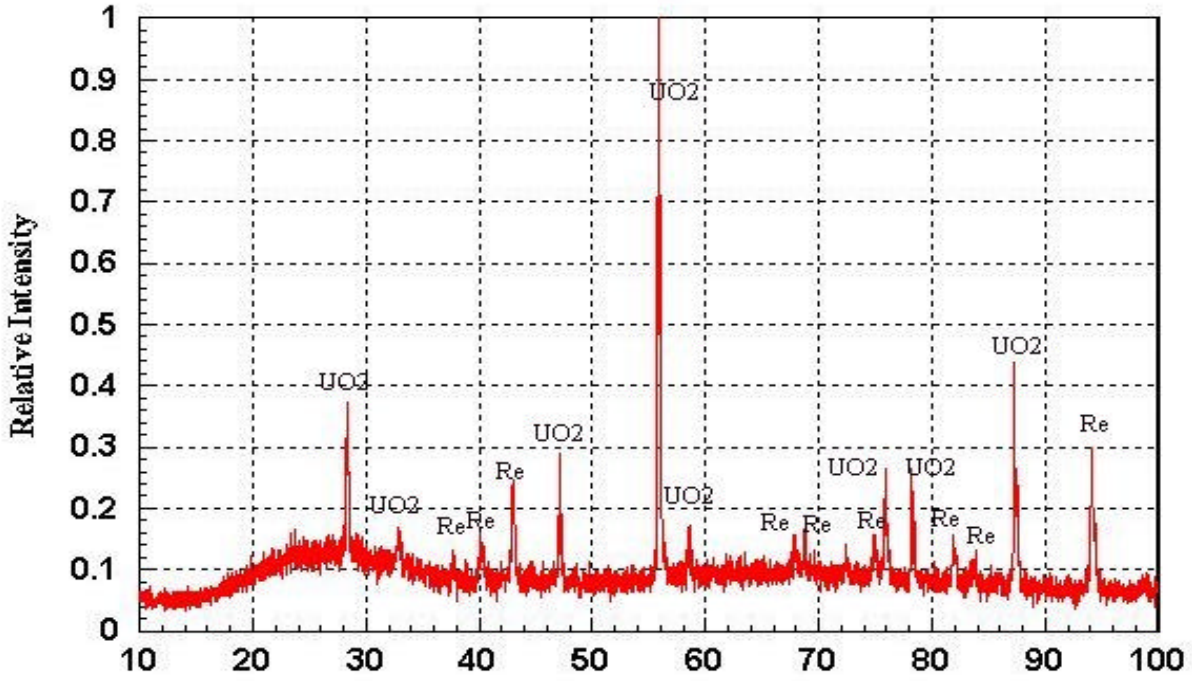

Figure 18: X-ray powder diffraction pattern of the middle region of the sample.

Furthermore, Backscattered Scanning Electron (BSE) images of the samples whose spectrums are shown above are represented in Figures 19 and 20. These images provide a qualitative map of the sample's chemical composition. This is due to proportionality between the average atomic number of the elements in an area scanned for the image and the yield of backscattered electrons. Lighter colored parts of the image correspond to areas of higher average atomic number (Z). Although uranium (Z=92) is greater than rhenium (Z=75), the lighter colored areas in Figures 19 and 20 correspond to Re since the average atomic number is lower for UO_2 containing oxygen atoms (Z=8).

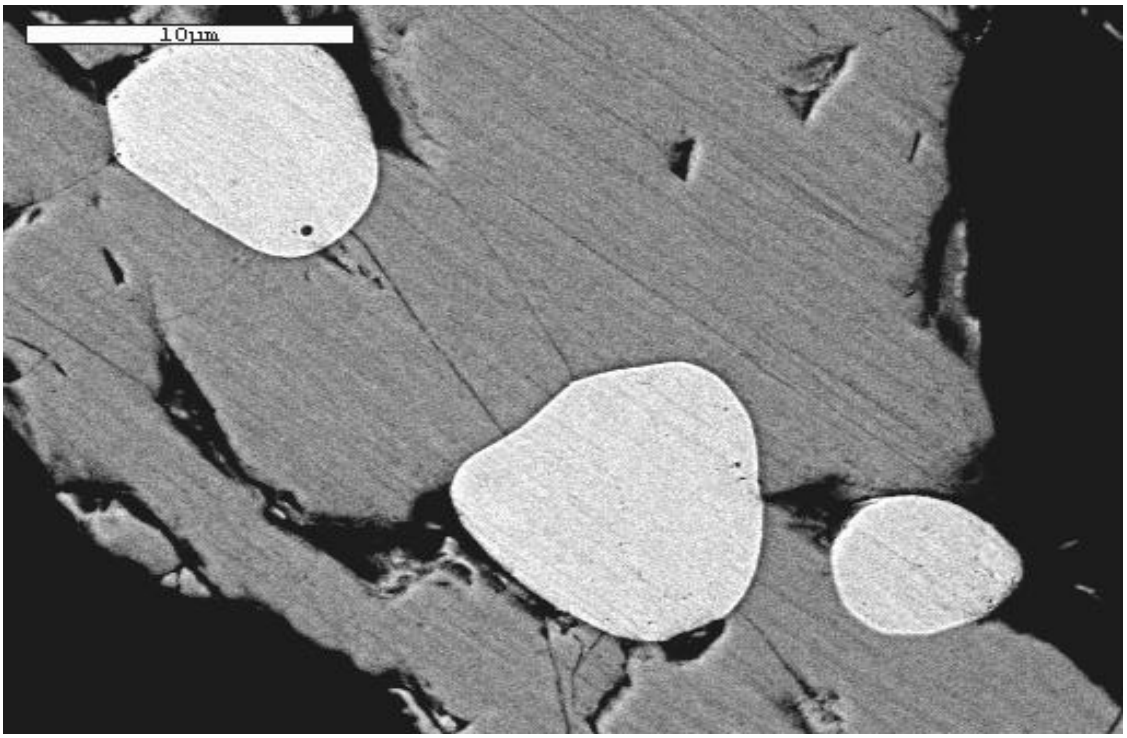

Figure 19: Back-scattered scanning electron micrograph showing compositional contrast of Re-UO_2 powders sintered for 10 hr. at 2500 K.

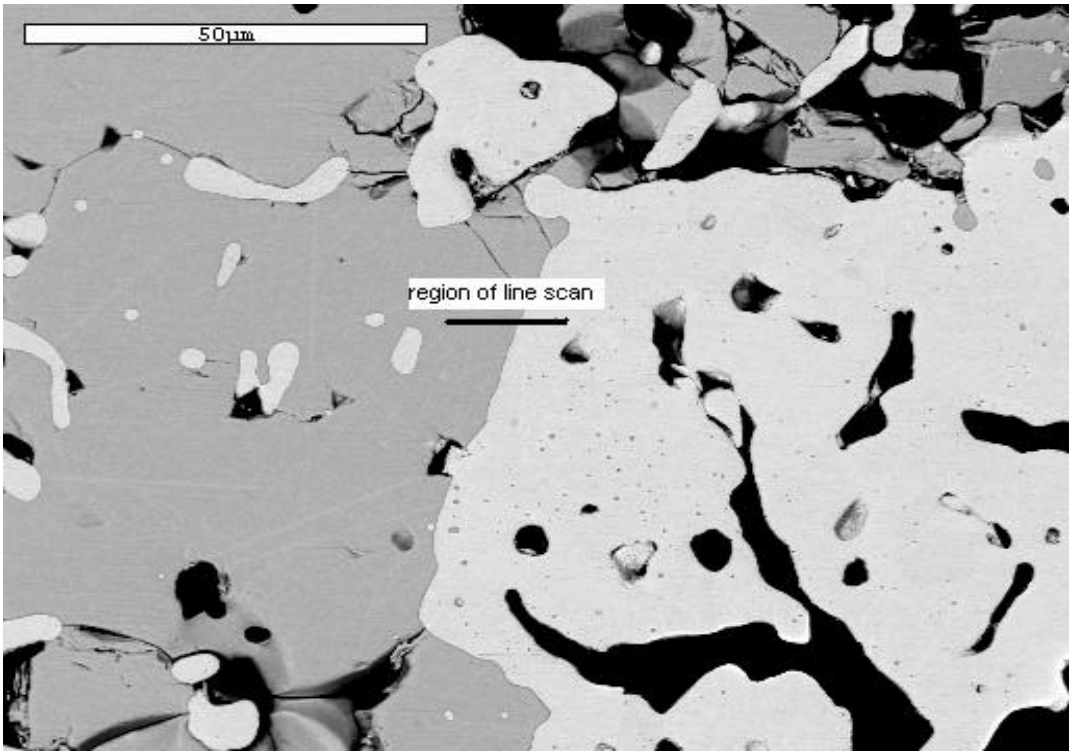

Figure 20: Back-scattered scanning electron micrograph showing compositional contrast of Re-UO_2 powders sintered for 10 hr. at 2500 K.

The interface between the Re and UO_2 regions is clear, sharp and distinct. EDS of the different regions confirmed that the lighter colored regions are unreacted rhenium. Line scans across these regions and their interface show sharp discontinuities at the interface indicating practically no interdiffusion of the elements, and no mixed phase. The region of the line scan is indicated on Figure 20, which is a picture of the middle part of the sample. It was operated from left to right on the sample. The corresponding line-scan graph itself is given in Figure 21. Once again, it appears clearly that the light phase is the rhenium phase and the darker one is the uranium dioxide.

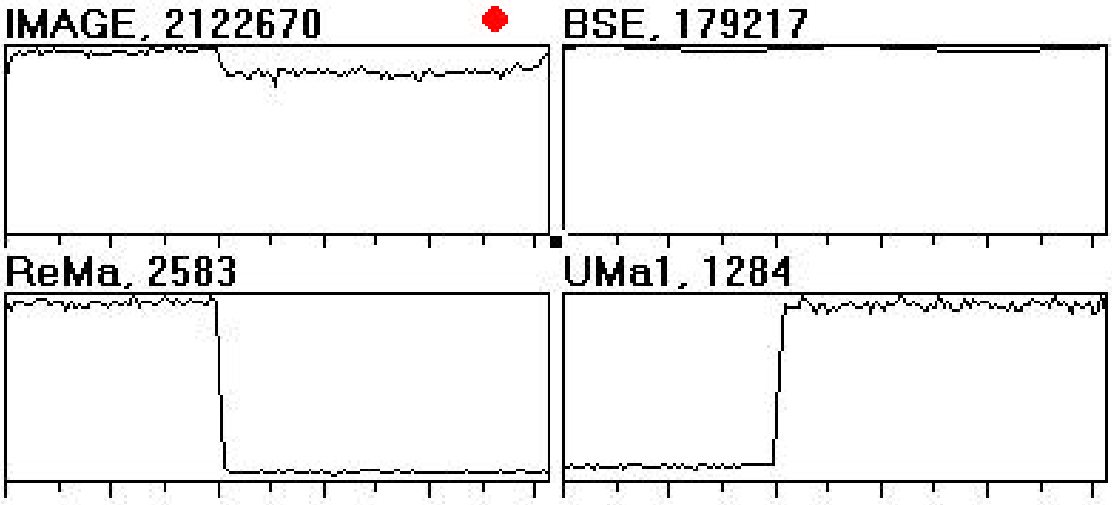

Figure 21: Line scan operated across the region showed on Figure 19.

Conclusions

Attention should be brought on the intrinsic difficulty to carry out high temperature corrosion and materials compatibility. Due to the high probability of reaction of chamber wall, heating elements, inductive coils, and residual gases, chemical isolation

of the test chamber is a challenging task. Although special efforts were made to keep an inert atmosphere in the furnace chamber by purging the system with helium gas, preventing oxygen ingression proved to be a daunting task. The presence of even low concentration of oxygen in the system could potentially make the chemical compatibility results useless. Another complication is the possible vaporization of UO_2 at the top surface of crucible. The electron-beam-welding technique that could have been well for such experiments was not available. Electron-beam welding of crucibles required pre-sintering and melting of the samples before the crucibles could actually be sealed. This would have required reaching extremely high temperatures with the same equipment available (with the same problems of potential external leaks.) This obviously could have defeated the purpose of the experiment.

As a conclusion, it should be reminded that the thermodynamic analysis suggests that, in the temperature range of interest [2000 K-3000 K], oxygen reacts with rhenium and forms volatile Re_2O_7. However, when uranium is present in the system, rhenium does not form any stable oxide because uranium dioxide has a much lower Gibbs free energy of formation than any of rhenium oxides. Therefore UO_2 is the most stable phase; it is not expected to react with Re at temperatures up to 3000 K. Experiment at 2500 K for ten hours confirms the thermodynamic analysis results that suggest full chemical compatibility of rhenium with UO_2 at temperatures up to 3000 K.

APPENDIX A
X-RAY POWDER DIFFRACTION ANALYSIS

The three-dimensional structure of non-amorphous materials is defined by regular, repeating planes of atoms that form a crystal lattice. When a focused X-ray beam interacts with these planes of atoms, part of the beam is transmitted, part is absorbed by the sample, part is refracted and scattered, and part is diffracted. Diffraction of an X-ray beam by a crystalline solid is analogous to diffraction of light by droplets of water, producing the familiar rainbow. X-rays are diffracted by each material differently, depending on what atoms make up the crystal lattice and how these atoms are arranged.

In X-ray powder diffractometry, X-rays are generated within a sealed tube that is under vacuum. A current is applied that heats a filament within the tube; the higher the current the greater the number of electrons emitted from the filament. This generation of electrons is analogous to the production of electrons in a television picture tube. A high voltage, typically 15-60 kilovolts, is applied within the tube. This high voltage accelerates the electrons, which then hit a target, commonly made of copper. When these electrons hit the target, X-rays are produced. The wavelength of these X-rays is characteristic of that target. These X-rays are collimated and directed onto the sample, which has been ground to a fine powder (typically to produce particle sizes of less than 10 microns). A detector detects the X-ray signal; the signal is then processed either by a microprocessor or electronically, converting the signal to a count rate. Changing the

angle between the X-ray source, the sample, and the detector at a controlled rate between preset limits is an X-ray scan.

When an X-ray beam hits a sample and is diffracted, we can measure the distances between the planes of the atoms that constitute the sample by applying Bragg's Law. Bragg's Law is:

$$n\lambda = 2d\sin\theta$$

where the integer n is the order of the diffracted beam, λ is the wavelength of the incident X-ray beam, d is the distance between adjacent planes of atoms (the d-spacings), and θ is the angle of incidence of the X-ray beam. Since we know λ and we can measure θ, we can calculate the d-spacings. The geometry of an XRD unit is designed to accommodate this measurement (fig. 1). The characteristic set of d-spacings generated in a typical X-ray scan provides a unique "fingerprint" of the mineral or minerals present in the sample. When properly interpreted, by comparison with standard reference patterns and measurements, this "fingerprint" allows for identification of the material.

APPENDIX B
ENERGY-DISPERSIVE X-RAY SPECTROMETRY (EDS)

In a SEM, when the incoming electron beam strikes the sample being analyzed, not only does it give secondary electrons and backscattered electrons, (which are used for imaging), it also generates characteristic x-rays. Indeed, those x-rays result from the incoming electrons knocking inner shell electrons out of atoms in the sample. As outer electrons drop into the vacancy, they are obliged to dispose of the excess energy, often as an x-ray photon. Since each element has its own set of energy levels, the emitted photons are indicative of the element that produced them. Analyzers are then used to characterize the x-ray photons for their energy (or wavelength) and abundance to determine the chemistry of sample.

EDS operates by using a crystal of silicon or germanium to detect the x-rays. Each photon generates multiple electron-hole pairs equal in total energy to the energy of the photon (each pair has a fixed energy determined by the crystal). A voltage is applied to the crystal to separate the electrons and holes so that the charges appear as a small step-change in voltage. Pre-amplifiers and amplifiers process the signal and pass it to a multichannel analyzer (i.e., analog-to-digital converter) so that the x-ray spectrum can eventually be displayed as a histogram of x-ray intensity as a function of energy.

The detector crystal is kept under vacuum at liquid nitrogen temperatures. It thus requires a window of some kind to isolate it from the SEM chamber. Early windows were made out of beryllium, but severely attenuated x-rays from elements lighter than sodium.

Improvements in materials has led to a generation of "thin-window" detectors which can pass x-rays down to and including boron. This is a great help when analyzing minerals (O) and organic compounds (C and O).

Types of X-ray Analyses

X-ray analyses may be broadly divided in to qualitative and quantitative analyses. Qualitative analyses are those that are concerned with determining the elements in a sample and perhaps a rough measures of their abundance, especially as trends across a sample. Qualitative analyses would thus include survey analyses, line-scan profiles, and x-ray maps. Quantitative analyses have as their goal the determination of the elemental composition at one or more points. There are a number of requirements that must be met for quantitative analyses to succeed. These analyses are discussed below.

Survey analyses

These analyses answer the general question "What is it?" They are useful if there is little hint of the composition of an unknown sample. These analyses seek to determine the elements present and their distribution. Spectra are collected for a number of points and the elements present are identified. Digital beam control allows users to probe around areas in a digital image to identify the various features and to check for consistency.

X-ray maps

Mapping generates a two-dimensional image using the abundance of an element as the intensity of the image. It easily shows where an element is and is not. Mapping only works for elements that have been specified. Therefore, it is first necessary to determine which elements are present by the use of a survey analysis. Mapping has come

a long way in recent years with digital beam control and faster electronics. Now, maps for multiple elements can be collected rapidly so that users get an idea of the elemental distribution in just a few minutes instead of the hours that used to be required. It is also often possible to combine x-ray maps to get even better ideas of the relative distribution (complementary or correlating) of elements.

Line-scan profiles

Similar to x-ray maps, this technique plots the abundance of an element with distance along a line rather than as intensity over a two-dimensional image. It is especially helpful for examining trends at interfaces and concentration gradients within a sample.

Quantitative Analysis

This involves careful determination of the identification and abundances of the elements present in a sample. Accuracy is often possible to tenths of a percent when standards are used. Standardless analyses can generally provide a compositional estimate, but with less accuracy. Several requirements must be met to ensure the success of a quantitative analysis. Samples must generally be flat, homogenous, and thick to satisfy assumptions in the analysis software. Standards are advisable to account for particular characteristics of the microscope. And all elements should be measurable.

Relative x-ray intensity varies with the angle of the surface of the sample. Therefore, the surface must at least be at some known, consistent angle if not altogether flat.

Correction algorithms assume a uniform distribution of elements on an atomic scale. Therefore, it is not possible to guarantee results when the excited volume is not uniform as in the case of dendritic structures or mixtures of particles.

Algorithms assume that electrons penetrate and are completely absorbed in the sample (i.e., not escaping from the underside). Likewise, samples must also be homogenous with depth so that the beam is entirely contained in a single phase.

APPENDIX C
SAMPLE 3

Sample 3 was a sample processed in a similar way to samples 1 and 2. It was meant to be run at 2600 K for one hundred hours. However, after 35 hours of experiment, the furnace arced; and the run was stopped. After analysis, it was found that the tungsten crucible had melt at some point and a protuberance built up outside. This actually diminished the distance separating the coil from the conductive crucible. At one point, this distance was short enough to trigger an arc between the coil and the crucible, which resulted in piercing the coil. Water came into the system, which obviously constituted a source of oxidation.

A blue deposit was observed on the walls of the furnace chamber, as well as some multicolor precipitate around the coil. Pictures of the system are provided in this appendix (Figures 22 and 23). The sample was submitted to x-ray powder diffraction analysis, and the obtained patterns are given below (Figures 24 and 25).

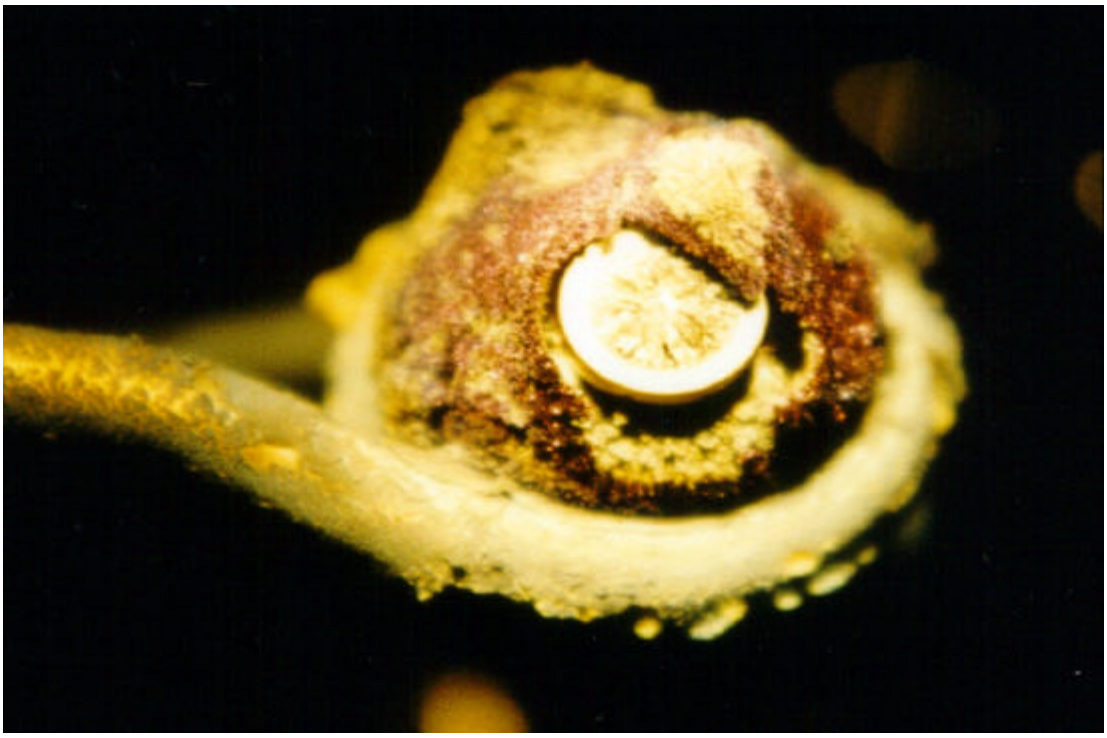

Figure 22: Crucible cap surrounded by oxide deposits.

Figure 23: Coil after removal; a blue-black deposit on the walls was observed similar to the deposit.

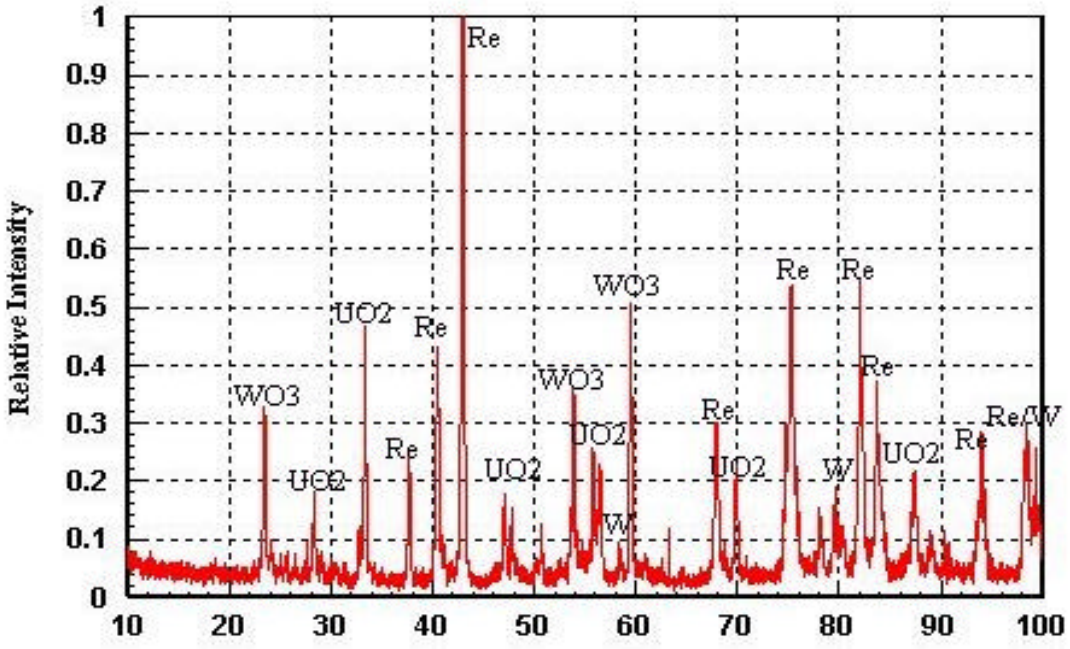

Figure 24: X-ray analysis pattern of the top part of the failed sample.

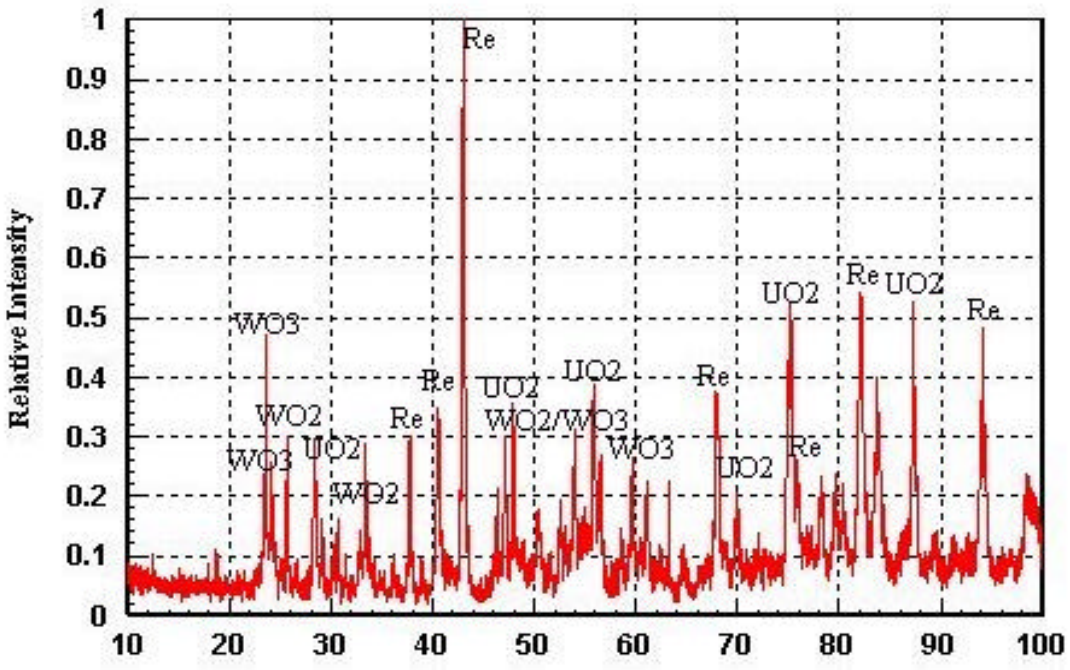

Figure 25: X-ray analysis pattern of the bottom region of the sample.

LIST OF REFERENCES

1. D. Buden, Summary of Space Nuclear Reactor Power Systems (1983-1992), in A Critical Review of Space Nuclear Power and Propulsion 1984-1993, edited by Mohamed S. El Genk, AIP Press, Woodbury, NY, 1994

2. General Electric, Nuclear Materials and Propulsion Operation, "710 High Temperature Gas Reactor, Program Summary Report, Volume III-Fuel Element Development," Report GEMP 600.

3. R. E. Latta and R. E. Fryxell, Determination of Solidus-Liquidus Temperatures in the UO_{2+x} System ($-0.50<x<0.20$)," Journal of Nuclear Materials 35 (1970), pp 195-210.

4. Povarova and M.A. Tylkina, "Physicochemical Pinciples of the Design of Rhenium Alloys," (paper presented at the International Symposium on Rhenium and Rhenium Alloys, Orlando, 1997), in Rhenium and Rhenium alloys edited by B.D. Bryskin, TMS, Warrendale, PA, 1996.

5. R. R. Jensen, "Materials Performance Issues in the Design of Fuel Elements for Externally Fueled Thermionic Hybrid Systems," CONF 940101, American Institute of Physics, pp 1525-1533.

6. B. D. Bryskin, "Evaluation of Properties and Special Features for High-Temperature Applications of Rhenium," CONF 920104, American Institute of Physics, pp 278-291.

7. R.W. Buckman, Jr, "Rhenium as an Alloy Addition to the Group VA Metals" (paper presented at the International Symposium on Rhenium and Rhenium Alloys, Orlando, 1997), in Rhenium and Rhenium alloys edited by B.D. Bryskin, TMS, Warrendale, PA, 1996.

8. B. Fischer, D. Freund, D. F. Lupton, "Stress-Rupture strength of Rhenium at Very High Temperatures", (paper presented at the International Symposium on Rhenium and Rhenium Alloys, Orlando, 1997), in Rhenium and Rhenium alloys edited by B.D. Bryskin, TMS, Warrendale, PA, 1996.

9. F. Habashi, "Rhenium Seventy Years Old" (paper presented at the International Symposium on Rhenium and Rhenium Alloys, Orlando, 1997), in Rhenium and Rhenium alloys edited by B.D. Bryskin, TMS, Warrendale, PA, 1996.

10. J. A. Mullendore, “Tungsten: Its Manufacture, Properties, and Application,” Refractory Metals and Their Industrial Applications, ASTM STP 849, R. E. Smallwood, Ed., American Society for Testing and Materials, Philadelphia, 1984, pp. 82-105.

11. J. W. Pugh, “Refractory Metals: Tungsten, Tantalum, Columbium, and Rhenium” (conference held in Cleveland, Ohio, April 16-17, 1957), in High Temperature Materials edited by R. F. Hehemann and G. Mervin Ault, Wiley, New York, 1959.

12. J. M. Stuve and M. J. Ferrante, “Thermodynamic Properties of Rhenium Oxides, 8 to 1400 K,” Bureau of Mines, 1976.

13. N. V. Sidgwick, Chemical Elements and their Compounds, vol II,Clarendon Press, Oxford, 1950.

14. S. Prakash, Advanced Chemistry of Rare Elements, Chemical Publishing Company, Inc, New York, 1967.

15. T. W. Knight, D. Kaoumi, S. Anghaie, “Study of the Chemical Compatibility of Uranium Dioxide with Rhenium,” STAIF-2001, Abuquerque, edited by Mohamed S. El Genk.

.

BIOGRAPHICAL SKETCH

Djamel Kaoumi was born on March 28, 1977 in Marseille (France). He went to the Marcel Pagnol high-school in Marseille, where he graduated with his French "baccalaureat" in sciences with honors. In 1997, he entered the French engineering school "Ecole Nationale Superieure de Physique de Grenoble" (ENSPG), part of the "Institut National Polytechnique de Grenoble" (INPG). In 1999, he decided to seize the opportunity to come to the United States as part of an exchange program with the University of Florida. In 2000, he graduated with his French engineering diploma in the field of physics sciences with a specialty in nuclear engineering (with honors). He has been in the United States to complete his degree of Master of Science in nuclear engineering sciences with a minor in materials science and engineering. He has also been working at the Innovative Nuclear Space Power Institute (INSPI) since 1999 as a graduate research assistant.